

Washington University School of Medicine

Digital Commons@Becker

---

2020-Current year OA Pubs

Open Access Publications

---

1-20-2023

## A pleiotropic chemoreceptor facilitates the production and perception of mating pheromones

Cassandra L Vernier  
*Washington University in St. Louis*

Nicole Leitner  
*Washington University in St. Louis*

Kathleen M Zelle  
*Washington University in St. Louis*

Merrin Foltz  
*Washington University in St. Louis*

Sophia Dutton  
*Washington University in St. Louis*

*See next page for additional authors*

Follow this and additional works at: [https://digitalcommons.wustl.edu/oa\\_4](https://digitalcommons.wustl.edu/oa_4)



Part of the [Medicine and Health Sciences Commons](#)

Please let us know how this document benefits you.

---

### Recommended Citation

Vernier, Cassandra L; Leitner, Nicole; Zelle, Kathleen M; Foltz, Merrin; Dutton, Sophia; Liang, Xitong; Halloran, Sean; Millar, Jocelyn G; and Ben-Shahar, Yehuda, "A pleiotropic chemoreceptor facilitates the production and perception of mating pheromones." *iScience*. 26, 1. 105882 (2023).  
[https://digitalcommons.wustl.edu/oa\\_4/2282](https://digitalcommons.wustl.edu/oa_4/2282)

This Open Access Publication is brought to you for free and open access by the Open Access Publications at Digital Commons@Becker. It has been accepted for inclusion in 2020-Current year OA Pubs by an authorized administrator of Digital Commons@Becker. For more information, please contact [vanam@wustl.edu](mailto:vanam@wustl.edu).

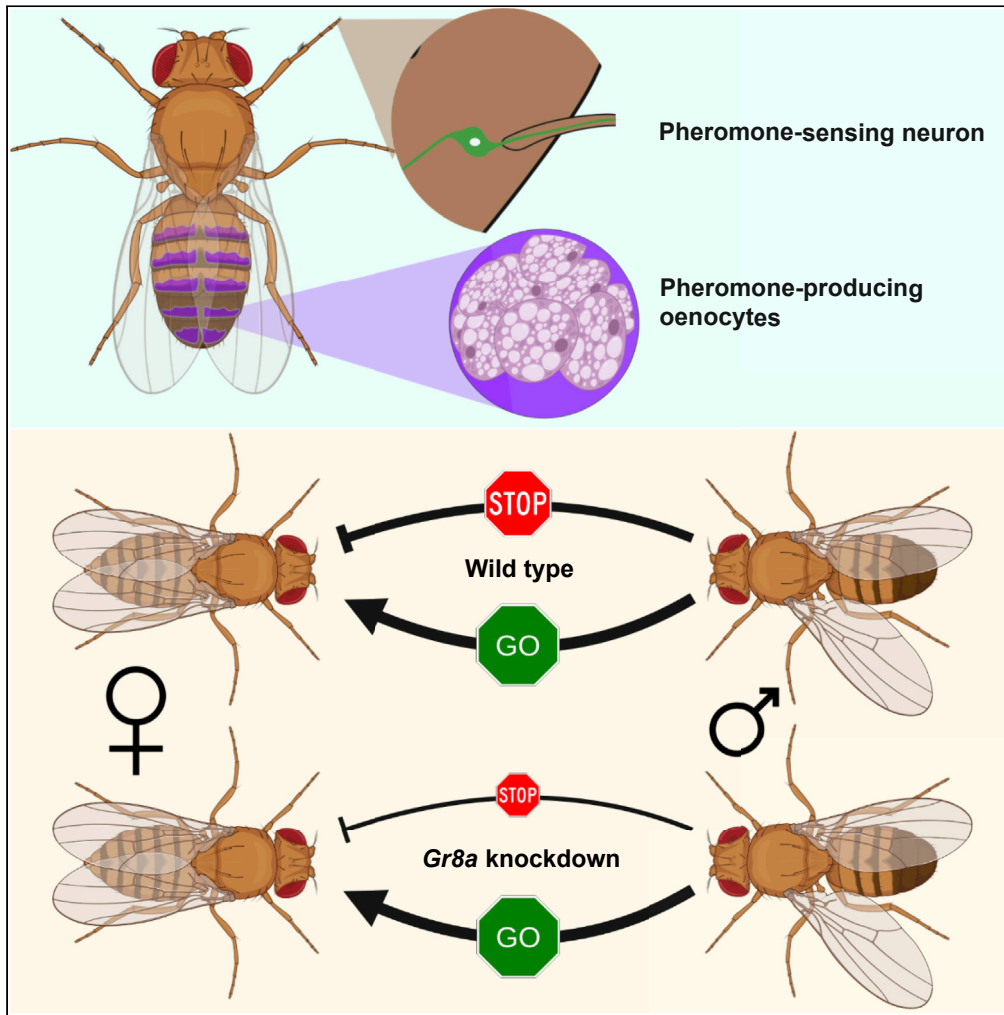
---

**Authors**

Cassandra L Vernier, Nicole Leitner, Kathleen M Zelle, Merrin Foltz, Sophia Dutton, Xitong Liang, Sean Halloran, Jocelyn G Millar, and Yehuda Ben-Shahar

Article

# A pleiotropic chemoreceptor facilitates the production and perception of mating pheromones



Cassandra L. Vernier, Nicole Leitner, Kathleen M. Zelle, ..., Sean Halloran, Jocelyn G. Millar, Yehuda Ben-Shahar

benshahary@wustl.edu

Highlights

*Gr8a* is enriched in gustatory receptor neurons and male pheromone-producing cells

*Gr8a* activity is required in females to appropriately respond to male pheromones

*Gr8a* mutant males do not respond to post-mating inhibitory signals in females

Male pheromone profiles are regulated by *Gr8a*

Vernier et al., iScience 26, 105882  
January 20, 2023 © 2022 The Authors.  
<https://doi.org/10.1016/j.isci.2022.105882>



## Article

## A pleiotropic chemoreceptor facilitates the production and perception of mating pheromones

Cassondra L. Vernier,<sup>1,4,6</sup> Nicole Leitner,<sup>1,6</sup> Kathleen M. Zelle,<sup>1,6</sup> Merrin Foltz,<sup>1</sup> Sophia Dutton,<sup>1</sup> Xitong Liang,<sup>2,5</sup> Sean Halloran,<sup>3</sup> Jocelyn G. Millar,<sup>3</sup> and Yehuda Ben-Shahar<sup>1,7,\*</sup>

## SUMMARY

**Optimal mating decisions depend on the robust coupling of signal production and perception because independent changes in either could carry a fitness cost. However, since the perception and production of mating signals are often mediated by different tissues and cell types, the mechanisms that drive and maintain their coupling remain unknown for most animal species. Here, we show that in *Drosophila*, behavioral responses to, and the production of, a putative inhibitory mating pheromone are co-regulated by *Gr8a*, a member of the *Gustatory receptor* gene family. Specifically, through behavioral and pheromonal data, we found that *Gr8a* independently regulates the behavioral responses of males and females to a putative inhibitory pheromone, as well as its production in the fat body and oenocytes of males. Overall, these findings provide a relatively simple molecular explanation for how pleiotropic receptors maintain robust mating signaling systems at the population and species levels.**

## INTRODUCTION

The majority of sexually reproducing animals use intricate mating signaling systems to find and evaluate potential mates. These systems rely on the robust physiological coupling between the production and perception of species-specific signals since any independent changes in either the signal or the capacity to sense it would carry a fitness cost.<sup>1–9</sup> Previously published theoretical models have postulated that the maintenance of robust coupling between the production and perception of mating signals is driven by either strong genetic linkage between the cellular and physiological processes that regulate mating-signal production and its perception, or via the action of pleiotropic genes that control both processes.<sup>1,5,10–12</sup> Consequently, both mechanisms provide plausible explanations for how mating-signaling systems could remain stable and reliable at the population level while still retaining their capacity for future diversification, as necessitated for speciation.<sup>3,5,12–16</sup>

Empirical data in support of the contribution of gene-linkage or pleiotropy to the maintenance of coupling between mating signal production and perception at the population level are rare.<sup>3,5,12,13,16</sup> For example, the complex characteristics of mating behaviors, and the species-specific signals that drive them, present a major barrier for identifying the actual molecular mechanisms and candidate pleiotropic genes that support the coupling between the production and perception of specific mating signals.<sup>4,17</sup> Moreover, how the functional coupling of the physiological processes responsible for the production and perception of mating signals remains robust is particularly puzzling since their perception is mediated by the peripheral sensory nervous system, while their production is restricted to specialized, non-neuronal pheromone producing cells.<sup>18–20</sup> Notwithstanding, a previous *Drosophila* study has implied that the gene *desat1*, which encodes a fatty acid desaturase, directly contributes to both the perception and production of pheromones.<sup>21</sup> However, whether the effect of *desat1* mutations on the behavioral response to pheromones is directly mediated via the modulation of pheromone perception by sensory neurons, or due to other non-neural effects, remains unknown. Consequently, the molecular identities of genes that may mediate the genetic and functional linkage between the production of insect mating pheromones by the oenocytes, and their perception by the chemosensory system, remained unknown.

Here we show that some pheromone-driven mating behaviors in *Drosophila* are regulated by the pleiotropic action of *Gr8a*, a member of the *Gustatory receptor* gene family,<sup>22,23</sup> which likely contributes to

<sup>1</sup>Department of Biology, Washington University in Saint Louis, 1 Brookings Drive, Saint Louis, MO 63130, USA

<sup>2</sup>Department of Neuroscience, Washington University School of Medicine, 660 South Euclid Avenue, St. Louis, MO 63110, USA

<sup>3</sup>Department of Entomology, University of California, Riverside, 900 University Avenue, Riverside, CA 92521, USA

<sup>4</sup>Present address: Carl R. Woese Institute for Genomic Biology, University of Illinois, 1206 W. Gregory Dr., Urbana, IL 61801, USA

<sup>5</sup>Present address: School of Life Sciences, Peking University, Beijing 100871, China

<sup>6</sup>These authors contributed equally

<sup>7</sup>Lead contact

\*Correspondence:

benshahar@wustl.edu

<https://doi.org/10.1016/j.isci.2022.105882>



the perception of inhibitory mating signals in pheromone-sensing neurons, and independently, to the production of inhibitory mating pheromones in non-neuronal abdominal pheromone-producing oenocytes. Together, these data provide a relatively simple molecular explanation for how genetic linkage could maintain functional coupling between the independent cellular and physiological processes that drive pheromone perception and production.

## RESULTS

### Some gustatory-like receptors exhibit enriched expression in abdominal tissues

Similar to other insect species, *Drosophila* cuticular hydrocarbons (CHCs), which are long-chain fatty acids synthesized by the fat body and oenocytes,<sup>24,25</sup> provide a hydrophobic desiccation barrier, as well as play an important role as pheromones in regulating diverse behaviors, including mating.<sup>18,20,26,27</sup> Specifically, complex blends of CHCs are often utilized by insects to communicate sex identity and female mating status, as well as to define the behavioral reproductive boundaries between closely related species.<sup>18,19,24,28–32</sup>

While some of the genes and pathways that contribute to CHC synthesis in *Drosophila* are known,<sup>19,20,26,27,33</sup> the molecular identities of most pheromonal CHC receptors remain unknown. Current models stipulate that the perception of volatile pheromones is mediated by olfactory sensory neurons (ORNs) located in the antennae and maxillary palps, while less volatile pheromones, such as CHCs, are sensed by specialized gustatory-like receptor neurons (GRNs) in the appendages (legs and wings), female genitalia, and the proboscis.<sup>30,31,34–43</sup> Indeed, several *Gustatory receptor* (*Gr*) gene family members have already been implicated in the detection of specific excitatory and inhibitory pheromones in *Drosophila*,<sup>44–47</sup> and the majority of genes that encode *Gr* gene family members are already known to be enriched in GRNs.<sup>48–51</sup>

Consequently, we chose to examine members of the *Gr* gene family as candidate pleiotropic genes that might contribute to both the perception and production of pheromonal mating signals in *Drosophila*. To begin to test this, we reasoned that any pleiotropic *Gr* genes, in addition to being expressed in the appendages and proboscis, should also be expressed in the abdominal oenocytes.<sup>24</sup> We tested this by using an RT-PCR screen, which revealed that 24 out of the 60 members of the *Gr* family are expressed in abdominal tissues of adult *Drosophila* (Table 1). This suggests that at least some *Gr* genes may contribute to both the perception and production of mating signals in *Drosophila*.

### *Gr8a* is a chemosensory receptor with sexually dimorphic expression in abdominal cells

Although several members of the *Gr* gene family, including *Gr68a*, *Gr32a*, *Gr66a*, *Gr39a*, and *Gr33a*, were previously linked to the sensory perception of mating pheromones,<sup>44–47,52</sup> none of these candidate genes were identified in our initial RT-PCR screen for *Gr* genes expressed in abdominal tissues of either males or females (Table 1). However, *Gr8a*, which was indicated by our screen as being a male-specific abdomen-enriched receptor (Table 1),<sup>53</sup> was previously shown to play a role in the chemosensation of the non-proteinogenic amino acid L-Canavanine.<sup>22,23</sup> Because our initial expression screen was based on whole-abdomen RNAs, we next used a GAL4 transgenic driver to label *Gr8a* in order to determine which cells likely express *Gr8a*. We found that, as was previously reported,<sup>22</sup> *Gr8a*-Gal4 labels 14–16 GRNs in the proboscis (Figures 1A and 1B), as well as two paired GRNs in the pretarsus of the prothoracic legs in males (Figure 1C) and females (Figure 1D). We also observed that *Gr8a*-Gal4 labels abdominal oenocyte-like cells in males (Figure 1E) but not females (Figure 1F). This male-biased *Gr8a* expression in the abdomen was further supported by qRT-PCR analysis (Figure 1G). Likewise, single-cell sequencing indicates that *Gr8a* is expressed in the male and female bitter taste bristles, gustatory receptors, oenocytes, and male reproductive system (Table 2).<sup>54</sup> These data further indicate that in addition to its chemosensory functions, *Gr8a* may also contribute to oenocyte and male reproductive physiology.

Next, we used a membrane-bound GFP reporter to trace the axonal projection patterns of *Gr8a*-Gal4 labeled GRNs in the nervous system and the prothoracic legs. Within the nervous system, both males and females displayed a subset of *Gr8a*-Gal4 labeled neurons in the abdominal neuromere of the ventral nerve cord (VNC), and two *Gr8a*-Gal4 labeled neurons in each prothoracic neuromere (Figures 1H–1M). In contrast to other GRN populations that display sexually dimorphic axonal projections in the VNC, such as the pheromone sensitive *pickpocket 23* (*ppk23*)-expressing neurons,<sup>30,31,41,42</sup> the axons of tarsal *Gr8a*-Gal4 labeled neurons ascend to the brain similarly in both males and females and do not cross the midline of the

**Table 1. Candidate *Gr* genes expressed in male and/or female abdomens**

Gene	Male	Female
<i>Gr2a</i>	–	+
<i>Gr8a</i>	+	–
<i>Gr10a</i>	+	+
<i>Gr21a</i>	–	+
<i>Gr22a</i>	+	–
<i>Gr22e</i>	+	+
<i>Gr36c</i>	+	–
<i>Gr58c</i>	+	+
<i>Gr59a</i>	+	+
<i>Gr59b</i>	+	+
<i>Gr63a</i>	+	–
<i>Gr64a</i>	+	–
<i>Gr64b</i>	+	+
<i>Gr64c</i>	+	+
<i>Gr64d</i>	+	–
<i>Gr66a</i>	+	+
<i>Gr89a</i>	+	+
<i>Gr93a</i>	–	+
<i>Gr93d</i>	+	+
<i>Gr97a</i>	+	+
<i>Gr98a</i>	+	+
<i>Gr98b</i>	–	+
<i>Gr98c</i>	+	+
<i>Gr98d</i>	+	+

Plus and minus signs indicate whether the expected endpoint RT-PCR products were respectively present or absent on an agarose gel. Only genes with positive PCR products in at least one sex are shown.

VNC in both sexes (Figures 1H–1K). Overall, these data indicate a lack of neuronal sexual dimorphism. Within the prothoracic legs, *Gr8a*-Gal4 labeled GRNs do not overlap with the sex determination factor *fru* (Figure 1N) or the ion channel *ppk23* (Figure 1O), which were previously shown to be expressed in pheromone-sensing GRNs in the fly appendages.<sup>31</sup> However, previous studies have shown that *Gr8a* is co-expressed with other pheromone-sensing neurons in the prothoracic legs and proboscis, including *Gr33a*, *Gr39a* and *Gr66a*.<sup>23,55</sup> Together, these data indicate that *Gr8a*-labeled GRNs likely represent a subclass of GRNs that is not sexually dimorphic, and has a similar expression pattern as some pheromone-sensing neurons.

To localize the expression of *Gr8a* in male-specific tissues, we imaged *Gr8a*-Gal4 labeled cells in the male reproductive system and abdomen. Within the male reproductive system, we found that *Gr8a*-Gal4 labeled cells are found in the seminal vesicles (Figures 2A–2C), the columnar cells comprising the exterior of the ejaculatory bulb, and in the cells near the duct leading from the ejaculatory bulb to the male genitalia (Figures 2D, 2F, and 2G). Interestingly, immunohistochemical staining of an endogenous GFP-tagged allele of *Gr8a* with an anti-GFP antibody indicates that the *Gr8a* protein is enriched in the basal surface of the columnar cells of the ejaculatory bulb, and seemingly collects where the ejaculatory bulb meets the ejaculatory duct (Figures 2E–2G), suggesting a role for *Gr8a* in the ejaculatory functions of male flies. In *Drosophila*, it is common for males to transfer pheromones to females during mating.<sup>36,38,45,56–61</sup> Therefore GR8A's localization pattern in the ejaculatory bulb could be consistent with a role in the transfer of pheromones during mating. In the male abdomen, we found that *Gr8a*-Gal4 labeled cells overlap with the oenocyte-specific *desat1* driver,<sup>24</sup> and are also found in *desat1*-negative fat body-like cells (Figures 2H–2J). Immunohistochemical staining of abdominal tissues from *Gr8a*-GFP males with an anti-GFP antibody revealed that the *Gr8a* protein is enriched in some oenocyte clusters

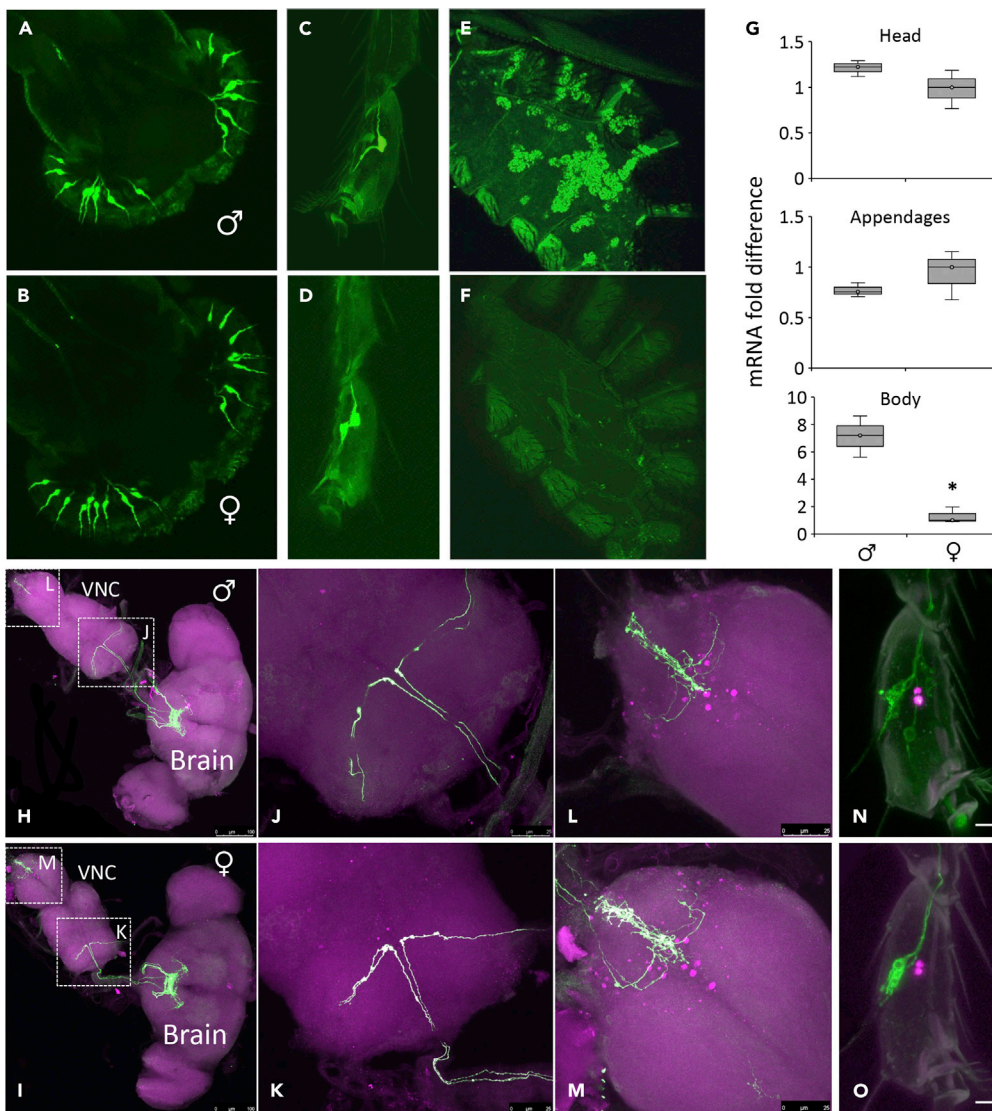


**Figure 1. *Gr8a* is a chemosensory receptor with sexually dimorphic expression in abdominal tissues**  
(A–F) *Gr8a*-Gal4 labels cells in the proboscis (A and B) and prothoracic legs (C and D) of both males (top) and females (bottom), but only labels cells in the abdomen of males (E and F).  
(G) *Gr8a* has sexually dimorphic mRNA expression in the bodies of flies. Relative mRNA levels were measured by real-time quantitative RT-PCR. Head:  $p = 0.215$ , Student's *t* test; Appendages:  $p = 0.377$ , Student's *t* test; Body:  $p = 0.008$ , Student's *t* test. Depicted as boxplots with inner points plotted, whiskers represent the minimum and maximum values,  $n = 3$ /group.  
(H–L) Axonal projection patterns in the ventral nerve cord (VNC) (dorsal view) and brain (anterior view) of a *Gr8a*-GAL4>UAS-CD8::GFP (green) male (H, J, and L) and female (I, K, and M). Magenta, neuropil marker (nc82). Scale bars in H–I = 100  $\mu$ m. Scale bars in J–M = 25  $\mu$ m.  
(N and O) *Gr8a*-Gal4 labeled GRNs are distinct from *ppk23* and *fru* pheromone sensing neurons. (N) Confocal z stack of a male *fruP1*-LexA>LexAop-myrGFP (green); *Gr8a*-GAL4>UAS-Red-Stinger (magenta) prothoracic leg. Scale bar = 50  $\mu$ m (O) Confocal z stack of a male *ppk23*-LexA>LexAop-CD8::GFP (green); *Gr8a*-GAL4>UAS-Red-Stinger (magenta) prothoracic leg. Scale bar = 50  $\mu$ m.

(Figure 2K). Although not directly tested here, this punctate expression pattern (Figure 2K) is consistent with the expression pattern of internal membrane lipid droplets associated with the fat body.<sup>62</sup> Compared to the expression pattern of the *Gr8a* protein in the ejaculatory bulb, the sub-cellular localization of *Gr8a* appears to differ depending on cell type. Together, these data indicate that in addition to its role in the perception of L-Canavanine, *Gr8a* may also contribute to the production of male mating pheromones.

**Table 2. Gr8a single-cell sequencing data<sup>54</sup>**

Tissue	Sex	Cell cluster name	Average expression	Percent expression
Whole body	Mixed	ejaculatory bulb	3.03861	46.0096
Whole body	Mixed	secretory cell of the male reproductive tract	1.41146	29.9728
Whole body	Mixed	seminal vesicle	0.233372	7.26257
Whole body	Mixed	bitter-sensitive labellar taste bristle	0.341535	5.96026
Whole body	Mixed	gustatory receptor neuron of the labellum	0.580359	5.47945
Whole body	Mixed	male reproductive tract muscle	0.237696	4.28571
Whole body	Mixed	epidermal cell of the abdominal posterior compartment	0.446717	2.94118
Whole body	Mixed	male accessory gland main cell	0.119238	2.28603
Whole body	Mixed	epidermal cell that specialized in antimicrobial response	0.257374	2.1093
Whole body	Mixed	male accessory gland secondary cell	0.0516077	2.01342
Whole body	Mixed	cyst cell branch b	0.0172017	1.60772
Whole body	Mixed	spermatid	0.092183	1.57846
Whole body	Mixed	spermatocyte cyst cell branch b	0.0208268	1.39535
Whole body	Mixed	cyst cell branch a	0.0144526	1.33779
Whole body	Mixed	spermatocyte cyst cell branch a	0.0100769	1.01833
Male reproductive glands	Male	ejaculatory bulb	3.16643	47.7803
Male reproductive glands	Male	secretory cell of the male reproductive tract	2.07202	44
Male reproductive glands	Male	seminal vesicle	0.233372	7.26257
Male reproductive glands	Male	male reproductive tract muscle	0.237696	4.28571
Male reproductive glands	Male	unannotated	0.220085	4
Male reproductive glands	male	spermatid	0.209198	3.68664
Male reproductive glands	male	hemocyte	0.0787541	2.77778
Male reproductive glands	male	male accessory gland main cell	0.119238	2.28603
Male reproductive glands	male	male accessory gland secondary cell	0.0516077	2.01342
Male reproductive glands	male	epithelial cell	0.0618365	1.52144
Oenocyte	mixed	ejaculatory bulb	0.452608	10.1852
Oenocyte	mixed	epithelial cell	0.313589	1.84697
Proboscis&maxillary palps	mixed	bitter-sensitive labellar taste bristle	0.341535	5.96026
Proboscis&maxillary palps	mixed	gustatory receptor neuron of the labellum	0.580359	5.47945
Testis	male	Cyst cells	0.0484747	3.2967
Testis	male	cyst cell branch b	0.0172017	1.60772
Testis	male	spermatocyte cyst cell branch b	0.0208268	1.39535
Testis	male	cyst cell branch a	0.0144526	1.33779
Testis	male	spermatocyte cyst cell branch a	0.0100769	1.01833

Tissue, tissue at which level the analysis was performed. Cell cluster name, cell cluster identified via marker expression. Average expression, average normalized expression of Gr8a in that cell cluster. Percent expression, percent of cells in that cell cluster that indicate enriched Gr8a expression. Only data indicating >1% percent expression shown.

### Gr8a activity in neuronal cells contributes to mating decisions in females

We next hypothesized that if Gr8a is a pleiotropic gene that independently contributes to the production of a mating pheromone in males, and its chemosensory perception in females, then the knockout of Gr8a in either males or females should have similar effects on female mating behavior. To test this, we first investigated whether Gr8a and the GRNs that express it, are required for sensory functions associated with female mate



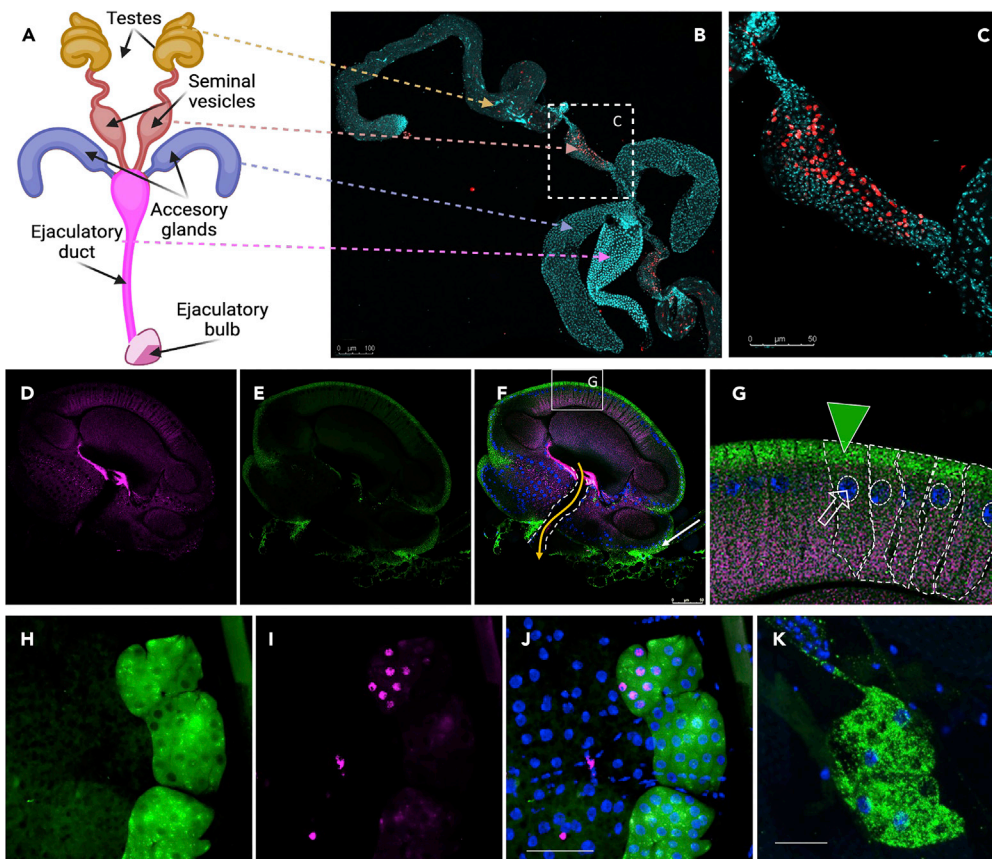


**Figure 2. *Gr8a* is enriched in the male reproductive system and abdominal cells**

(A) Depiction of the male reproductive system.

(B and C) *Gr8a*-Gal4 labels cells in the seminal vesicles. Confocal z stack images of a *Gr8a*-GAL4>UAS-Red-Stinger (red) male reproductive system. Turquoise, nuclear marker (DAPI). Scale bar in B = 100  $\mu$ m. Scale bar in C = 50  $\mu$ m.

(D–G) *Gr8a*-Gal4 labeled cells and the GR8A protein are enriched in the ejaculatory bulb. Confocal z stack image of the ejaculatory bulb in a *Gr8a*-GFP; *Gr8a*-GAL4>UAS-CD4::tdTomato male: (D) *Gr8a*-Gal4 (magenta); (E) GFP-tagged *Gr8a* (green); (F) Merge. GR8A protein is enriched where the ejaculatory duct meets the ejaculatory bulb (white arrow). Yellow arrow, duct leading from the ejaculatory bulb to the male genitalia. Scale bar = 50  $\mu$ m. (G) Inset of F. GR8A protein is enriched along the basal surface of ejaculatory bulb columnar cells. White dashed lines, outline of individual cells; green arrow, GR8A protein sub-cellular localization; white arrow, nucleus of cell; blue, nuclear marker (DAPI).

(H–J) *Gr8a*-Gal4 labels oenocytes and other abdominal cells. Confocal z stack images of oenocytes in a *Gr8a*-GAL4>UAS-CD8::GFP; *desat1*>*luciferase* male: (H) *desat1* (green); (I) *Gr8a* (magenta); (J) Merge. Blue, nuclear marker (DAPI). Scale bar = 50  $\mu$ m.

(K) GR8A protein is enriched in abdominal cells. Confocal z stack of a GFP-tagged *Gr8a* allele in male abdominal cells; green, anti-GFP; blue, nuclear marker (DAPI). Scale bar = 50  $\mu$ m.

choice by using single-pair courtship assays.<sup>30,31</sup> To do this, we blocked neuronal transmission in female *Gr8a*-Gal4 expressing neurons through the transgenic expression of tetanus toxin (TNT), which specifically affects synaptic function by cleaving neuronal synaptobrevin.<sup>63</sup> We found that *Gr8a*-Gal4>UAS-TNT females had shortened copulation latency relative to wild-type females, when courted by wild-type males (Figure 3A), while male-based courtship decisions, including courtship latency and courtship index, were unaffected (Figure S1). Similarly, homozygous (Figures 3B and 3C) and hemizygous (Figure 3C) *Gr8a*-null females exhibited shorter copulation latencies compared to control females when courted by wild-type males, which can be partially rescued by driving the expression of the *Gr8a* cDNA by *Gr8a*-GAL4 (Figure 3D). In contrast, genetic manipulations of *Gr8a* in males did not affect male courtship behavior as measured by courtship latency and index toward wild-type females (Figure S1). However, wild-type virgin females exhibited shorter copulation latencies toward *Gr8a* mutant males relative to wild-type controls (Figure 3E), suggesting that the *Gr8a* mutant males are more attractive to females than wild-type controls.

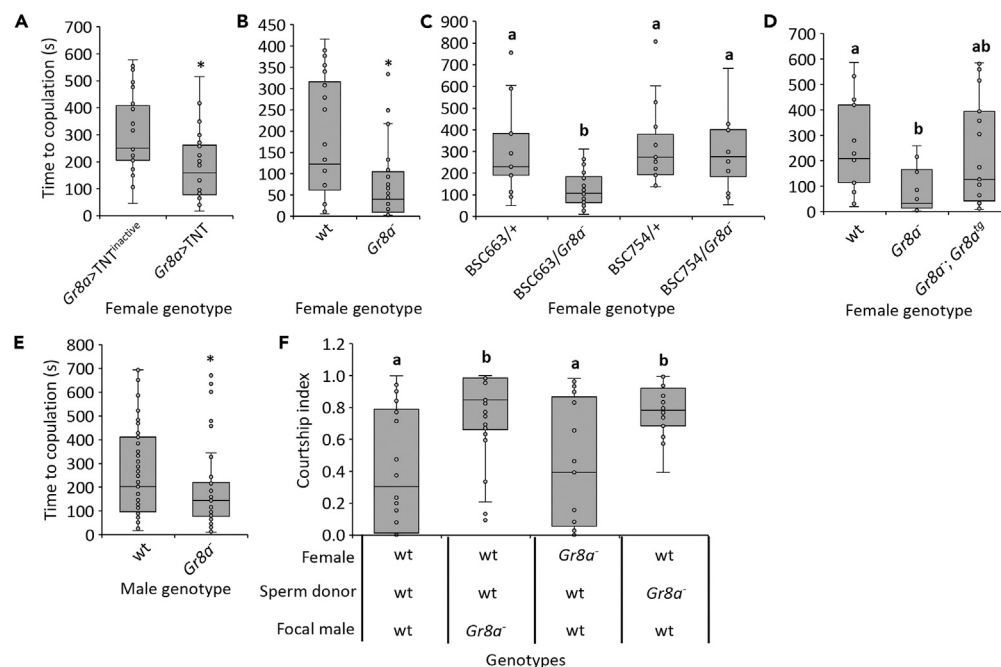


**Figure 3. *Gr8a* activity contributes to the perception and production of an inhibitory signal associated with mating decisions in males and females**

(A) Blocking neural activity in female *Gr8a*-labeled sensory neurons (*Gr8a>TNT*) shortens copulation latency relative to wild-type controls (*Gr8a>TNT<sup>inactive</sup>*),  $p = 0.008$ , Student's *t* test.

(B) Homozygous *Gr8a* null females show shortened copulation latency relative to wild-type controls,  $p = 0.009$ , Mann-Whitney Rank-Sum Test.

(C) Homozygous and hemizygous *Gr8a* null females show shortened copulation latency relative to wild-type controls,  $p = 0.0006$ , Kruskal-Wallis Test. Letters above bars indicate statistically significant Dunn's Test with FDR  $p$  value adjustment contrasts between groups. *Df(1)BSC663* is a deficiency that covers the *Gr8a* locus. *Df(1)BSC754* was used as a control.

(D) Expression of *Gr8a* cDNA with the *Gr8a* promoter (*Gr8a<sup>-</sup>;Gr8a<sup>19</sup>*) rescues the copulation latency phenotype in *Gr8a* mutant females,  $p = 0.022$ , Kruskal-Wallis Test. Letters above bars indicate statistically significant Dunn's Test with FDR  $p$  value adjustment contrasts between groups.

(E) Wild-type females exhibit shortened copulation latency when courted by *Gr8a* mutant males relative to wild-type males,  $p = 0.048$ , Mann-Whitney Rank-Sum Test.

(F) *Gr8a* mutant males do not recognize the mating status of females, and have a reduced effect on female post-mating attractiveness,  $p = 0.004$ , Kruskal-Wallis Test. Letters above bars indicate statistically significant Dunn's Test with FDR  $p$  value adjustment contrasts between groups. Female, female genotype; Sperm donor, genotype of males mated first with focal females; Focal male, genotypes of experimental males presented with mated females. All assays performed under red light conditions. All data depicted as boxplots with inner points and outliers plotted, whiskers represent the minimum and maximum values,  $n > 12$ /group. See [Data S1](#) "P-value data" for exact  $p$  values.

While we do not use techniques such as electrophysiology to specifically test if *Gr8a*-labeled neurons respond to pheromones, these behavioral data are consistent with *Gr8a* regulating female mating decisions via the detection of male-borne mating pheromones. Furthermore, the shortened copulation latency by *Gr8a*-silenced and mutant females and the increased attractiveness of *Gr8a* mutant males may suggest that *Gr8a* plays a role in the production of and behavioral response to a male-produced inhibitory mating pheromone. This inhibitory role may be considered analogous to *Gr8a*'s previously known role in taste aversion.<sup>22,23</sup>

### **Gr8a regulates the post-mating perception and attractiveness of females**

Mating decisions in *Drosophila* rely on a balance between excitatory and inhibitory drives.<sup>24,35,64–66</sup> In *Drosophila melanogaster*, previous studies showed that, in order to increase their fitness, males transfer inhibitory mating pheromones to females during copulation, which subsequently lowers the overall attractiveness of mated females to other males.<sup>36,38,45,56–61</sup> Because our behavioral data indicate that *Gr8a* plays a role in female mating decisions, possibly through the production and behavioral response

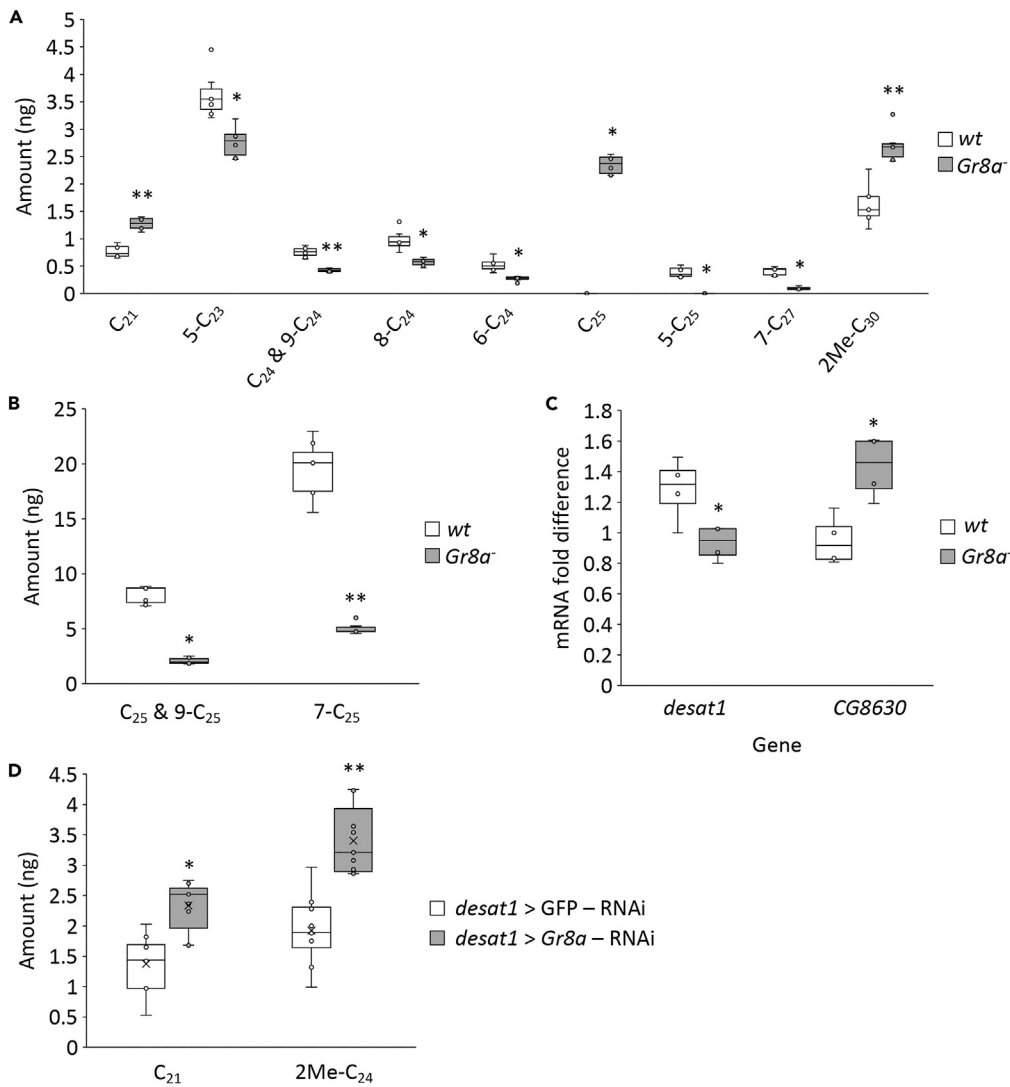


**Figure 4. *Gr8a* mutation and knock-down affect the pheromone profiles of males**

(A and B) Wild-type (wt) and *Gr8a* mutant (*Gr8a*<sup>-</sup>) males differ in the relative abundance of individual CHCs. (A) CHCs found in low amounts in males. (B) CHCs found in high amounts in males. Only affected CHCs are shown. See Table 3 for the complete list and exact p values. \*, p < 0.05, \*\*, p < 0.01, Student's t test or Mann Whitney Rank-Sum Test, n = 6 (*Gr8a*<sup>-</sup>) or 7 (wt).

(C) The *Gr8a* mutation affects the expression level of several desaturase genes in male abdomens. Only affected genes are shown. See Table 4 for the complete list and exact p values. \*, p < 0.05, Student's t test, n = 4/group.

(D) Control (*desat1* > GFP-RNAi) and oenocyte-specific *Gr8a* knockdown (*desat1* > *Gr8a*-RNAi) males differ in the relative abundance of individual CHCs. Only affected CHCs are shown. See Table 6 for the complete list and exact p values. \*, p < 0.05, \*\*, p < 0.01, Student's t test or Mann Whitney Rank-Sum Test, n = 10. All data depicted as boxplots with inner points and outliers plotted, whiskers represent the minimum and maximum values. Alkanes denoted as C<sub>n</sub>, where n denotes the number of carbon atoms in the chain. Alkenes denoted as N-C<sub>n</sub>, where N denotes the location of carbon-carbon double bond in chain. Methyl-branched alkanes denoted as NMe-C<sub>n</sub>, where N denotes the carbon in the chain at which the methyl branch occurs.

to male-produced inhibitory pheromones (Figures 3A–3E), we next tested whether *Gr8a* is involved in the transfer of inhibitory pheromones to females during copulation as measured by a decrease in post-mating female attractiveness. We found that *Gr8a* mutant males were more likely to court-mated females than wild-type controls (Figure 3F), suggesting that *Gr8a* is involved in the recognition of the inhibitory signals that label the post-mating status of females. We also found that wild-type males failed to recognize the

**Table 3. Male CHCs**

R.T.	Compound	wt amount (ng)	<i>Gr8a</i> <sup>-</sup> amount (ng)	p value	Adjusted p value
12.31	C <sub>21</sub>	0.770	1.275	<0.001	<0.001
13.24	Unknown	0.094	0.220	<0.001	<0.001
14.2	C <sub>22</sub>	1.170	1.098	0.720	1
14.34	7-C <sub>22</sub>	0.474	0.568	0.0264	0.660
15.25	Unknown	0.167	0.262	<0.001	0.005
16.22	C <sub>23</sub> & 9-C <sub>23</sub>	17.916	14.652	0.002	0.051
16.4	7-C <sub>23</sub>	39.561	41.105	0.525	1
16.53	5-C <sub>23</sub>	3.630	2.768	0.001	0.031
16.71	cVA	13.536	18.115	0.012	0.292
18.03	C <sub>24</sub> & 9-C <sub>24</sub>	0.757	0.425	<0.001	<0.001
18.19	8-C <sub>24</sub>	0.976	0.572	<0.001	0.017
18.27	7-C <sub>24</sub>	0.761	0.467	0.003	0.084
18.37	6-C <sub>24</sub>	0.521	0.270	<0.001	0.016
18.46	5-C <sub>24</sub>	0.057	0.055	0.773	1
19.09	2Me-C <sub>24</sub>	3.171	3.752	0.042	1
19.95	C <sub>25</sub>	0.000	2.350	0.001	0.036
20.02	C <sub>25</sub> & 9-C <sub>25</sub>	8.111	2.075	<0.001	<0.001
20.18	7-C <sub>25</sub>	19.401	5.028	<0.001	<0.001
20.42	5-C <sub>25</sub>	0.390	0.000	0.002	0.051
22.89	2Me-C <sub>26</sub>	7.857	8.005	0.680	1
23.7	C <sub>27</sub>	1.469	0.832	0.013	0.333
23.94	7-C <sub>27</sub>	0.403	0.097	<0.001	<0.001
26.46	2Me-C <sub>28</sub>	6.517	6.650	0.772	1
27.25	C <sub>29</sub>	0.456	0.365	0.191	1
29.89	2Me-C <sub>30</sub>	1.623	2.705	<0.001	0.002

Retention time (R.T.), relative abundance (ng), p value (Student's t-test or Mann Whitney Rank-Sum Test), and adjusted p value (Bonferroni correction) of each compound in each sample (5 flies per sample) for wild-type (wt) and *Gr8a* mutant (*Gr8a*<sup>-</sup>) males. x Alkanes denoted as C<sub>n</sub>, where n denotes the number of carbon atoms in the chain. Alkenes denoted as N-C<sub>n</sub>, where N denotes the location of carbon-carbon double bond in chain. Methyl-branched alkanes denoted as NMe-C<sub>n</sub>, where N denotes the carbon in the chain at which the methyl branch occurs. See [Data S1](#) "P-value data" for exact p values.

mating status of wild-type females that were previously mated with *Gr8a* mutant males ([Figure 3F](#)), indicating that *Gr8a* expression in sperm-donor males is also important in the post-mating attractiveness of females. Together, our behavioral studies are consistent with the pleiotropic role of *Gr8a* in the production of an inhibitory mating signal in the male oenocytes, which is transferred to females during copulation, and its behavioral response in both males and females.

### **Gr8a contributes to the pheromone profiles of males**

Because our data indicate that *Gr8a* mutant females have a lower copulation latency compared to control females, and *Gr8a* mutant males are unable to detect the mating status of females, we hypothesized that *Gr8a* contributes to the production and/or transfer of an inhibitory pheromone in males. Therefore, we next examined whether the *Gr8a* mutation has a direct effect on the CHC profiles of males and mated females. We found that the CHC profile of *Gr8a* mutant males is different from that of wild-type males ([Figures 4A](#) and [4B](#) and [Table 3](#)). In particular, the *Gr8a* mutation increases the levels of two alkanes and one methyl-branched alkane and decreases the levels of 8 alkenes ([Figures 4A](#) and [4B](#) and [Table 3](#)), including two compounds that have been identified as male sex compounds in *D. melanogaster*.<sup>27,67–69</sup>

Although the exact mechanism by which *Gr8a* might be regulating the levels of specific CHCs remains unknown, we found that the expression levels of the desaturases *desat1* and *CG8630*, which play a role in the

**Table 4. Desaturase gene expression**

Gene	wt mRNA fold difference	<i>Gr8a</i> <sup>-</sup> mRNA fold difference	p value
<i>desat1</i>	1.282	0.931	0.037
<i>desat2</i>	1.413	1.270	0.506
CG8630	0.951	1.429	0.012
CG9747	0.838	0.525	0.343
CG9743	1.060	0.959	0.373
CG15331	0.774	1.000	0.21

Relative mRNA expression of each desaturase gene for wild-type (wt) and *Gr8a* mutant (*Gr8a*<sup>-</sup>) males. Statistics via Student's t-test. See [Data S1](#) "P-value data" for exact p values.

biosynthesis of alkenes,<sup>18</sup> are affected by the *Gr8a* mutation in the male abdomen (Figure 4C and Table 4). Together, these data suggest that *Gr8a* action in oenocytes contributes to the production of some cuticular alkenes, alkanes, and methyl-branched alkanes in males, which possibly function as inhibitory mating pheromones.

Interestingly, we did not identify any individual CHCs that differed quantitatively between females that mated with *Gr8a* mutant males relative to those that mated with wild-type males (Table 5). This suggests that our analysis did not capture the transfer of an inhibitory pheromone, either because our analysis was not sensitive enough, because the pheromone is not a CHC, or because the behavioral effects seen above (Figure 3F) result from other post-mating responses that act independently of a transferred pheromone. At this time, we cannot discern between these possibilities. Therefore, we currently cannot definitively say whether *Gr8a* is involved in the transfer, in addition to the production, of a pheromone by males to females during copulation.

Since the *Gr8a* mutation is not spatially restricted in *Gr8a* mutant males, it is possible that at least some of the effects of the *Gr8a* mutation on the pheromone profiles of males are indirectly mediated via its action in GRNs, instead of directly mediated via its action in oenocytes. Therefore, we next examined the effect of oenocyte-specific *Gr8a* knockdown on the production of male CHCs. We found that oenocyte-specific *Gr8a* RNAi knockdown in males leads to significant changes in the abundance of two CHCs relative to control males (Figure 4D and Table 6). In contrast, fat body-specific knockdown of *Gr8a* has no effect on CHCs in males (Table 7). These data suggest that *Gr8a* is likely to play an oenocyte-specific role in the production of male CHCs. Together, our behavioral and pheromonal data indicate that *Gr8a* action contributes to mating decisions in females by co-regulating the behavioral response to an inhibitory mating pheromone by females and males, as well as its production in males. This is consistent with a pleiotropic function for *Gr8a*.

### Gr8a-associated cuticular hydrocarbons inhibit normal courtship behaviors

To further characterize whether any of the individual CHCs regulated by *Gr8a* function as inhibitory mating pheromones, we tested the effect of perfuming naive males with the synthetically available individual candidate CHCs identified in Figure 4 (Table S4) on the copulation latency of wild-type females.<sup>30,31,70–72</sup> We found that wild-type females did not copulate with *Gr8a* mutant males that were perfumed with exaggerated amounts of the alkenes 9-C<sub>25</sub>, 7-C<sub>25</sub>, and 7-C<sub>27</sub> (Figures S2A and S2B). Similarly, we found that wild-type males exhibited a longer courtship latency and lower courtship index toward wild-type females perfumed with an exaggerated amount of 9-C<sub>25</sub> (Figures S2C–S2E) and exhibited longer copulation latency toward wild-type females perfumed with an exaggerated amount of 7-C<sub>25</sub> (Figures S2F–S2H). In contrast, perfuming wild-type females with an exaggerated amount of 7-C<sub>27</sub> had no effect on male courtship or female mating latency (Figures S2I–S2K). Due to the possibility that exaggerated levels of CHCs may not have biologically relevant effects on behavior, we next perfumed males with biologically relevant amounts (comparable to those found on wild-type male flies) (Table S4) of two of the alkenes found to have an effect on female receptivity in Figures 6A and 6B. With these lower amounts, we found that wild-type females no longer responded differently to CHC perfumed and control males (Figure 5A). Likewise, *Gr8a* null mutant females did not respond differently to 7-C<sub>25</sub> perfumed and control males (Figure 5B). Interestingly, *Gr8a* null mutant females displayed a lower copulation latency toward 7-C<sub>27</sub> perfumed males compared to control males, suggesting that *Gr8a* is not necessary to sense this compound. While we do not yet know why

**Table 5. Mated-female CHCs**

R.T.	Compound	wt amount (ng)	<i>Gr8a</i> <sup>-</sup> amount (ng)	p value	Adjusted p value
12.31	C <sub>21</sub>	0.119	0.125	0.596	1
14.2	C <sub>22</sub>	0.167	0.179	0.308	1
14.34	7-C <sub>22</sub>	0.014	0.015	0.932	1
15.25	Unknown	0.121	0.104	0.178	1
16.09	C <sub>23</sub>	3.297	3.390	0.681	1
16.4	7-C <sub>23</sub>	1.249	1.392	0.045	1
16.39	7,11-C <sub>23</sub>	0.240	0.220	0.520	1
16.53	5-C <sub>23</sub>	0.129	0.120	0.380	1
16.71	cVA	0.680	0.587	0.292	1
17.99	C <sub>24</sub>	0.335	0.373	0.043	1
18.19	8-C <sub>24</sub>	0.079	0.088	0.109	1
19.09	2Me-C <sub>24</sub>	0.619	0.572	0.403	1
19.95	C <sub>25</sub>	2.786	2.938	1	1
20.02	C <sub>25</sub> & 9-C <sub>25</sub>	1.591	1.984	0.589	1
20.18	7-C <sub>25</sub>	1.602	1.531	0.370	1
20.25	7,11-C <sub>25</sub>	0.925	0.868	0.436	1
20.42	5-C <sub>25</sub>	0.268	0.284	0.223	1
20.47	5,9-C <sub>25</sub>	0.348	0.362	0.693	1
22.89	2Me-C <sub>26</sub>	0.048	0.047	0.481	1
23.7	C <sub>27</sub>	5.105	4.790	1	1
23.8	9-C <sub>27</sub>	1.849	1.685	0.937	1
23.94	7-C <sub>27</sub>	1.281	1.443	0.277	1
24.1	7,11-C <sub>27</sub>	1.972	2.505	0.353	1
24.28	5,9-C <sub>27</sub>	10.940	10.193	0.604	1
25.85	7,11-C <sub>28</sub>	1.306	1.257	0.915	1
26.46	2Me-C <sub>28</sub>	0.337	0.334	0.289	1
27.25	C <sub>29</sub>	2.430	2.579	0.008	0.244
27.7	7,11-C <sub>29</sub>	0.293	0.355	0.842	1
29.89	2Me-C <sub>30</sub>	9.950	10.150	0.127	1
31.03	7,11-C <sub>31</sub>	0.690	0.751	0.503	1

Retention time (R.T.), compound, relative abundance (ng), p value (Student's t-test or Mann Whitney Rank-Sum Test), and adjusted p value (Bonferroni correction) of each compound as part of the total pheromonal bouquet for females (5 flies per sample) mated with wild-type (wt) or *Gr8a* mutant (*Gr8a*<sup>-</sup>) males. Alkanes denoted as C<sub>n</sub>, where n denotes the number of carbon atoms in the chain. Alkenes denoted as N-C<sub>n</sub>, where N denotes the location of carbon-carbon double bond in chain. Methyl-branched alkanes denoted as NMe-C<sub>n</sub>, where N denotes the carbon in the chain at which the methyl branch occurs. See [Data S1](#) "P-value data" for exact p values.

*Gr8a* mutant females seemingly responded differently from wild-type females to 7-C<sub>27</sub>, our data indicate that although some of the CHCs regulated by *Gr8a* activity in the male oenocytes may function as inhibitory mating pheromones when present at exaggerated amounts, they may not have an effect at biologically relevant levels. This suggests that perfuming with small amounts of individual compounds is not sufficient to alter mating behaviors. Overall, these data suggest that the behavioral responses to the inhibitory mating pheromones regulated by *Gr8a* are complex and likely modulated by multiple receptors and multiple compounds acting in tandem.

### Variations in *Gr8a* contribute to species-specific male pheromonal profiles across the *Drosophila* genus

As populations diversify, pheromonal signals and their receptors often have to co-evolve to maintain behavioral species boundaries.<sup>1,8,73,74</sup> One possible mechanism for maintaining the functional coupling of coevolving

**Table 6. Oenocyte knockdown male CHCs**

R.T.	Compound	<i>desat1</i> > GFP-RNAi amount (ng)	<i>desat1</i> > <i>Gr8a</i> -RNAi amount (ng)	p value	Adjusted p value
12.31	C <sub>21</sub>	1.375	2.334	<0.001	0.027
13.24	Unknown	0.027	0.048	0.174	1
14.2	C <sub>22</sub>	1.299	1.308	0.951	1
14.34	7-C <sub>22</sub>	0.460	0.689	0.022	0.643
15.25	Unknown	0.175	0.401	<0.001	0.002
16.09	C <sub>23</sub>	10.094	6.741	0.152	1
16.22	C <sub>23</sub> & 9-C <sub>23</sub>	6.764	9.427	0.967	1
16.4	7-C <sub>23</sub>	33.537	43.029	0.183	1
16.53	5-C <sub>23</sub>	2.115	2.261	0.776	1
16.71	cVA	5.587	7.386	0.342	1
17.99	C <sub>24</sub>	0.424	0.310	0.049	1
18.03	C <sub>24</sub> & 9-C <sub>24</sub>	0.424	0.351	0.052	1
18.19	8-C <sub>24</sub>	0.864	0.721	0.414	1
18.27	7-C <sub>24</sub>	0.356	0.299	0.347	1
18.37	6-C <sub>24</sub>	0.335	0.356	0.757	1
18.46	5-C <sub>24</sub>	0.047	0.059	0.900	1
19.09	2Me-C <sub>24</sub>	1.924	3.400	<0.001	<0.001
19.95	C <sub>25</sub>	1.471	0.897	0.595	1
20.02	C <sub>25</sub> & 9-C <sub>25</sub>	1.822	0.916	0.438	1
20.18	7-C <sub>25</sub>	7.145	3.747	0.053	1
20.42	5-C <sub>25</sub>	0.490	0.290	0.141	1
20.47	C <sub>25</sub> diene	0.029	0.037	0.448	1
21.23	Unknown	0.260	0.206	0.190	1
22.89	2Me-C <sub>26</sub>	4.750	5.212	0.063	1
23.7	C <sub>27</sub>	0.396	0.291	0.086	1
23.94	7-C <sub>27</sub>	0.117	0.081	0.188	1
26.46	2Me-C <sub>28</sub>	2.766	2.739	0.825	1
27.25	C <sub>29</sub>	0.243	0.223	0.461	1
29.89	2Me-C <sub>30</sub>	0.735	0.692	0.671	1

Retention time (R.T.), average relative abundance (ng), p value (Student's t-test or Mann Whitney Rank-Sum Test), and adjusted p value (Bonferroni correction) of each compound in each sample (5 flies per sample) for control (*desat* > GFP-RNAi) and oenocyte-specific *Gr8a* knockdown (*desat* > *Gr8a*-RNAi) males. Alkanes denoted as C<sub>n</sub>, where n denotes the number of carbon atoms in the chain. Alkenes denoted as N-C<sub>n</sub>, where N denotes the location of carbon-carbon double bond in chain. Methyl-branched alkanes denoted as NMe-C<sub>n</sub>, where N denotes the carbon in the chain at which the methyl branch occurs. See [Data S1](#) "P-value data" for exact p values.

signal-receptor pairs during speciation is pleiotropy.<sup>1,4,12</sup> Because our data suggest that *Gr8a* is a pleiotropic pheromone receptor, we tested the hypothesis that cross-species variations in the *Gr8a* coding sequence may have contributed to the rapid evolution of mating pheromones in the *Drosophila* species group.<sup>73,75,76</sup> To test this hypothesis, we first performed a phylogenetic analysis of *Gr8a* orthologs across *Drosophila* species, which indicated that *Gr8a* is a conserved receptor across the *Drosophila* genus that has sexually dimorphic expression across *Drosophila* species (Figures 6A and 6B). Furthermore, the alignment of *Gr8a* proteins across all the major *Drosophila* clades revealed that, in spite of its high overall sequence conservation, the *Gr8a* receptor has at least one phylogenetically variable domain (magenta frame, Figure 6C), which includes the second intracellular and extracellular domains (Figure 6D).

Although the ligand-binding domains of the insect *Gr* gene family have not yet been identified, such a phylogenetically variable protein domain suggests that *Gr8a* may contribute to species-specific shifts in

**Table 7. Fat body knockdown male CHCs**

R.T.	Compound	<i>r4</i> > GFP-RNAi amount (ng)	<i>r4</i> > <i>Gr8a</i> -RNAi amount (ng)	p value	Adjusted p value
12.31	C <sub>21</sub>	5.919	5.651	0.796	1
13.24	Unknown	0.51	0.066	0.006	0.181
14.2	C <sub>22</sub>	6.358	7.061	0.579	1
14.34	7-C <sub>22</sub>	2.621	2.373	0.912	1
15.25	Unknown	0.657	0.594	0.798	1
16.09	C <sub>23</sub>	20.344	6.761	0.075	1
16.22	C <sub>23</sub> & 9-C <sub>23</sub>	56.899	57.616	0.393	1
16.4	7-C <sub>23</sub>	152.262	122.022	0.631	1
16.53	5-C <sub>23</sub>	8.632	8.482	0.796	1
16.71	cVA	26.28	34.567	0.441	1
17.99	C <sub>24</sub>	1.077	1.946	0.343	1
18.03	C <sub>24</sub> & 9-C <sub>24</sub>	2.053	2.201	0.631	1
18.19	8-C <sub>24</sub>	5.511	4.341	0.739	1
18.27	7-C <sub>24</sub>	2.358	1.699	0.473	1
18.37	6-C <sub>24</sub>	1.754	1.641	0.910	1
18.46	5-C <sub>24</sub>	0.217	0.38	0.099	1
19.09	2Me-C <sub>24</sub>	4.759	5.898	0.248	1
19.95	C <sub>25</sub>	1.572	4.029	0.571	1
20.02	C <sub>25</sub> & 9-C <sub>25</sub>	13.311	11.862	0.796	1
20.18	7-C <sub>25</sub>	51.387	32.153	0.529	1
20.42	5-C <sub>25</sub>	3.665	2.766	1	1
20.47	C <sub>25</sub> diene	0.011	0.09	0.101	1
21.23	Unknown	2.196	2.357	0.739	1
22.89	2Me-C <sub>26</sub>	15.24	17.021	0.481	1
23.7	C <sub>27</sub>	3.2	3.514	0.770	1
23.94	7-C <sub>27</sub>	1.32	0.834	0.597	1
26.46	2Me-C <sub>28</sub>	12.745	14.269	0.724	1
27.25	C <sub>29</sub>	1.482	1.299	0.657	1
29.89	2Me-C <sub>30</sub>	3.505	3.969	0.706	1

Retention time (R.T.), average relative abundance (ng), p value (Student's t-test or Mann Whitney Rank-Sum Test), and adjusted p value (Bonferroni correction) of each compound in each sample (5 flies per sample) for control (*r4* > GFP-RNAi) and fat-body-specific *Gr8a* knockdown (*r4* > *Gr8a*-RNAi) males. Alkanes denoted as C<sub>n</sub>, where n denotes the number of carbon atoms in the chain. Alkenes denoted as N-C<sub>n</sub>, where N denotes the location of carbon-carbon double bond in chain. Methyl-branched alkanes denoted as NMe-C<sub>n</sub>, where N denotes the carbon in the chain at which the methyl branch occurs. See [Data S1](#) "P-value data" for exact p values.

ligand-binding specificity and/or sensitivity across the *Drosophila* genus. Therefore, we next tested whether the transgenic rescue of the *Gr8a* null allele via ectopic expression of *Gr8a* cDNAs from different *Drosophila* species is sufficient to drive changes in the CHC profile of *D. melanogaster* males. By using a cross-species male mate-choice assay, we found that while *D. melanogaster* males are generally promiscuous, they do court *Drosophila mojavensis* females at a significantly lower proportion than conspecific females. Because these assays are performed under red light, which eliminates visual mating cues, these data suggested that the lower sex drives toward *D. mojavensis* females is likely pheromone-dependent ([Figure 6E](#)). Subsequently, we derived transgenic *D. melanogaster* lines which express either the *D. mojavensis* or the *D. melanogaster* *Gr8a* cDNAs driven by an oenocyte-specific GAL4 in the background of the *Gr8a* null allele. Comparison of male CHC profiles across the two genotypes revealed that rescuing the *Gr8a* mutation by *Gr8a* cDNAs from these two distantly related species resulted in significantly different male CHC profiles ([Figures 6F and 6G](#), [Table 8](#)). These data indicate that species-specific *Gr8a* coding variations are sufficient



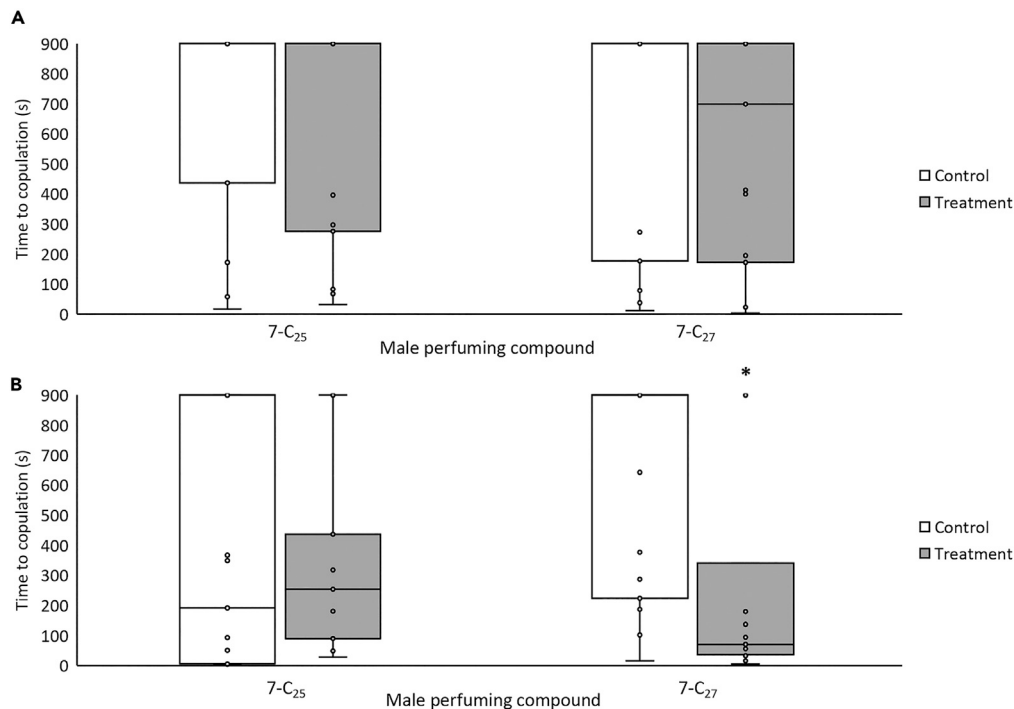


**Figure 5. *Gr8a*-associated alkenes inhibit normal courtship behaviors**

(A and B) Perfuming males with a biologically relevant amount of 7-C<sub>25</sub> does not affect copulation latency with wild-type females,  $p = 0.537$ , Mann Whitney Rank-Sum Test (A) or *Gr8a* mutant females,  $p = 0.691$ , Mann Whitney Rank-Sum Test (B). Perfuming males with a biologically relevant amount of 7-C<sub>27</sub> does not affect copulation latency with wild-type females,  $p = 0.463$ , Mann Whitney Rank-Sum Test (A), but does affect copulation latency with *Gr8a* mutant females,  $p = 0.008$ , Mann Whitney Rank-Sum Test (B). Depicted as boxplots with inner points and outliers plotted, whiskers represent the minimum and maximum values,  $n = 15$ /group. See [Data S1](#) "P-value data" for exact p values.

to drive differential CHC production by the male oenocytes, and suggest that pleiotropic chemoreceptors may have played a role in driving the rapidly evolving behavioral mating boundaries in *Drosophila*.

## DISCUSSION

The data presented here demonstrate that *Gr8a* is a pleiotropic chemoreceptor that co-regulates the perception and production of an inhibitory pheromonal signal that plays an important role in mating behaviors of both *D. melanogaster* sexes. How *Gr8a*, a member of a canonical chemoreceptor family, might also contribute to the production of pheromonal signals is not obvious. In some better understood secretory cell types, autoreceptors are essential for the regulation of synthesis and secretion rates. For example, dopaminergic and serotonergic cells regulate rates of synthesis and release of their respective neuromodulators by the action of autoreceptors.<sup>77,78</sup> These autoreceptors act via signaling feedback in response to changes in the extracellular concentrations of the secreted molecule.<sup>77,78</sup> Therefore, we hypothesize that *Gr8a* might regulate the synthesis and/or secretion of specific CHCs by acting as an oenocyte-intrinsic autoreceptor, which regulates the synthesis of specific CHCs by providing feedback information about their levels in internal stores and/or extracellularly (Figure 7).

Recent studies have indicated that *Drosophila* bitter receptor neurons typically express multiple *Gr* genes, and that bitter receptor ligand specificity is determined via combinatorial heteromeric receptor complexes.<sup>23,79,80</sup> *Gr8a* is specifically required for the sensory perception of the feeding deterrent L-canavanine,<sup>22,23</sup> but not for the detection of other bitter feeding deterrents such as caffeine, strychnine, and umbelliferone.<sup>81,82</sup> Our data indicate that similar to other *Drosophila* bitter taste receptors,<sup>46,52</sup> *Gr8a* contributes to inhibitory sensory inputs in the contexts of both feeding and mating decisions. In the context of feeding, *Gr8a*-dependent perception of L-canavanine is mediated via its heterotrimeric interaction with *Gr66a* and *Gr98b* in bitter sensing neurons in the proboscis.<sup>23</sup> However, while *Gr66a* and *Gr98b* were also identified in our initial screen for receptors enriched in the adult abdomen, we found that *Gr66a* is expressed in both sexes and *Gr98b* is specifically enriched

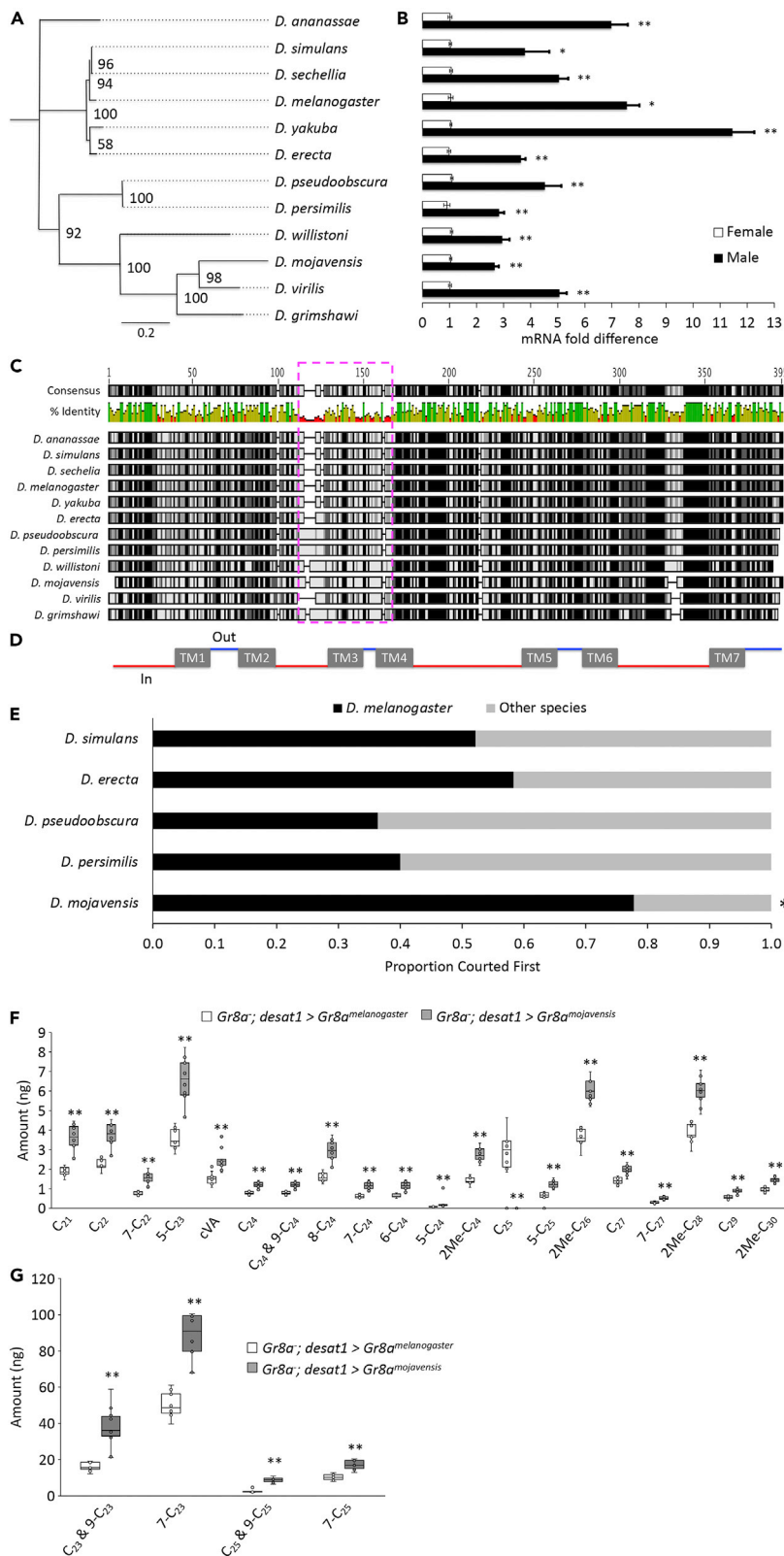


**Figure 6. Sexually dimorphic *Gr8a* expression across the *Drosophila* genus may contribute to species-specific differences in male CHC profiles**

(A) Phylogenetic tree of *Drosophila Gr8a* proteins. Substitution rate = 0.2.

(B) *Gr8a* mRNA expression is enriched in males relative to females across *Drosophila*. Black, males; white, females. \*,  $p < 0.05$ ; \*\*,  $p < 0.01$ ; Mann Whitney Rank-Sum Test,  $n = 4/\text{group}$ . Live *D. grimshawi* was not analyzed because live specimens were not available at the *Drosophila* Species Stock Center (DSSC).

(C) Multiple aligned amino acid sequences of *Gr8a* protein sequences from 12 species across *Drosophila*. The magenta dashed box highlights a putative hypervariable protein domain. Numbers on top of the alignment indicate amino acid number. Black, 100% identical; Dark Gray, 80–100% similar; Light Gray, 60–80% similar; White, less than 60% similar (Blosum62 score matrix, threshold = 1). Bars below consensus represent overall level of amino acid conservation.

(D) *Gr8a* protein topology. Boxes, transmembrane domains; Red lines, intracellular domain; Blue lines, extracellular domains.

(E) In female choice assays, *D. melanogaster* males court females from most other *Drosophila* species first at an equal proportion as *D. melanogaster* females, but court *D. mojavensis* females first at a lower proportion than *D. melanogaster* females. Assays performed under red light. \*,  $p < 0.05$ , Pearson's Chi-squared test.

(F and G) *Gr8a* mutant *D. melanogaster* males with oenocyte-specific *D. melanogaster Gr8a* rescue differ in the relative abundance of many CHCs from *Gr8a* mutant *D. melanogaster* males with oenocyte-specific *D. mojavensis Gr8a* rescue. (F) CHCs found in low amounts in males. (G) CHCs found in high amounts in males. Only affected CHCs are shown. See Table 8 for the complete list and exact p values. \*,  $p < 0.05$ , \*\*,  $p < 0.01$ , Student's t test or Mann Whitney Rank-Sum Test,  $n = 10$ . Depicted as boxplots with inner points and outliers plotted, whiskers represent the minimum and maximum values.

*Gr8a*; *desat1* > *Gr8a*<sup>*melanogaster*</sup>, *D. melanogaster Gr8a* oenocyte rescue; *Gr8a*; *desat1* > *Gr8a*<sup>*mojavensis*</sup>, *D. mojavensis Gr8a* oenocyte rescue. Alkanes denoted as C<sub>n</sub>, where n denotes the number of carbon atoms in the chain. Alkenes denoted as N-C<sub>n</sub>, where N denotes the location of carbon-carbon double bond in chain. Methyl-branched alkanes denoted as NMe-C<sub>n</sub>, where N denotes the carbon in the chain at which the methyl branch occurs. See Data S1 "P-value data" for exact p values.

in females (Table 1). Although *Gr66a* seems to be co-expressed with *Gr8a* in the foreleg,<sup>55</sup> due to these expression differences in the abdomen, we suspect that *Gr8a*-dependent contributions to sensory functions associated with mating decisions are independently driven via its heteromerization with different *Gr* genes than those that drive feeding-specific decisions.

Although we do not yet know the specific chemical identity of the ligand of *Gr8a*, previous studies indicated that at least two inhibitory mating pheromones, 11-cis-vaccenyl acetate (cVA) and CH503, are transferred from males to females during copulation. Since our data do not suggest that the *Gr8a* mutation affects the level of cVA expressed by males (Table 3), it is unlikely that the volatile cVA, which is known to act via the olfactory receptor *Or67d*,<sup>34,36,38</sup> is the putative *Gr8a* ligand. Likewise, it is unlikely that CH503 is the putative *Gr8a* ligand because CH503 has been reported to signal via *Gr68a*-expressing neurons, which have previously been shown to be anatomically distinct from the *Gr8a*-expressing GRNs we describe here (Figures 1 and 2).<sup>23,55,57,83</sup> Instead, our analyses of the effect of the *Gr8a* mutation on the CHC profile (Figure 4), and our results of the perfuming behavioral studies (Figure 5), suggest that a combination of other CHCs, possibly including the alkenes 9-C<sub>25</sub> and 7-C<sub>25</sub>, are the likely ligands of *Gr8a*.

Pleiotropic receptors may contribute to the physiological coupling between the production and perception of some mating pheromones by acting as both a sensory receptor in pheromone-sensing neurons and possibly as an autoreceptor for the same chemical in the pheromone-producing oenocytes. Overall, the simplest interpretation of our data is that *Gr8a* is one such pleiotropic receptor. Although we do not use electrophysiology to directly show that *Gr8a* expressing neurons respond to *Drosophila* pheromones, our imaging, behavioral and CHC data indicate that *Gr8a* is involved in the behavioral response to *Drosophila* inhibitory mating pheromones, as well as the production of the same chemical in the pheromone-producing oenocytes. Our finding that *Gr8a* displays sexually dimorphic expression that is conserved across the *Drosophila* genus, and has at least one phylogenetically variable domain (Figures 6A–6C), suggests that it might also drive the divergence of mating signaling systems in association with rapid speciation. This is supported by our finding that rescuing the *Gr8a* mutation specifically in *D. melanogaster* oenocytes with a *Gr8a* cDNA from a distant species, *D. mojavensis*, leads to the development of a male CHC profile that is different from the profile of mutant males rescued with the *D. melanogaster Gr8a* cDNA (Figures 6F and 6G).

Studies in other animal species suggest that receptor pleiotropy likely plays a role in mating signaling via other sensory modalities including auditory communication in crickets<sup>3,16,84</sup> and visual communication in fish.<sup>85</sup> While the specific genes and signaling pathways that mediate the coupling of the mating signals and their receptors in these mating systems remain mostly unknown, these data suggest that genetic

**Table 8. Oenocyte rescue male CHCs**

R.T.	Compound	<i>Gr8a</i> ; <i>desat1</i> > <i>Gr8a</i> <sup><i>melanogaster</i></sup> amount (ng)	<i>Gr8a</i> ; <i>desat1</i> > <i>Gr8a</i> <sup><i>mojavensis</i></sup> amount (ng)	p value	Adjusted p value
12.31	C <sub>21</sub>	1.888	3.597	<0.001	<0.001
13.24	Unknown	0.018	0.063	<0.001	<0.001
14.2	C <sub>22</sub>	2.256	3.744	<0.001	0.005
14.34	7-C <sub>22</sub>	0.752	1.539	<0.001	0.005
15.25	Unknown	0.158	0.317	<0.001	0.005
16.09	C <sub>23</sub>	10.509	0	0.002	0.064
16.22	C <sub>23</sub> & 9-C <sub>23</sub>	16.14	37.673	<0.001	<0.001
16.4	7-C <sub>23</sub>	50.584	87.714	<0.001	<0.001
16.53	5-C <sub>23</sub>	3.559	6.501	<0.001	0.005
16.71	cVA	1.519	2.484	<0.001	0.007
17.99	C <sub>24</sub>	0.782	1.192	<0.001	<0.001
18.03	C <sub>24</sub> & 9-C <sub>24</sub>	0.782	1.192	<0.001	<0.001
18.19	8-C <sub>24</sub>	1.599	2.926	<0.001	<0.001
18.27	7-C <sub>24</sub>	0.623	1.147	<0.001	0.005
18.37	6-C <sub>24</sub>	0.646	1.14	<0.001	0.005
18.46	5-C <sub>24</sub>	0.089	0.247	<0.001	0.005
19.09	2Me-C <sub>24</sub>	1.43	2.745	<0.001	0.005
19.95	C <sub>25</sub>	2.72	0	<0.001	0.007
20.02	C <sub>25</sub> & 9-C <sub>25</sub>	2.825	8.746	<0.001	0.005
20.18	7-C <sub>25</sub>	10.116	17.492	<0.001	<0.001
20.42	5-C <sub>25</sub>	0.63	1.223	<0.001	0.005
20.47	C <sub>25</sub> diene	0.012	0.007	0.480	1.000
21.23	Unknown	0.373	0.938	<0.001	<0.001
22.89	2Me-C <sub>26</sub>	3.652	6.04	<0.001	<0.001
23.7	C <sub>27</sub>	1.411	1.992	<0.001	0.001
23.94	7-C <sub>27</sub>	0.292	0.522	<0.001	<0.001
26.46	2Me-C <sub>28</sub>	3.863	6.011	<0.001	<0.001
27.25	C <sub>29</sub>	0.566	0.886	<0.001	<0.001
29.89	2Me-C <sub>30</sub>	0.942	1.445	<0.001	<0.001

Retention time (R.T.), average relative abundance (ng), p value (Student's t-test or Mann Whitney Rank-Sum Test), and adjusted p value (Bonferroni correction) of each compound in each sample (5 flies per sample) for *Gr8a* mutant *D. melanogaster* males with oenocyte-specific *D. melanogaster Gr8a* rescue (*Gr8a*; *desat1* > *Gr8a*<sup>*melanogaster*</sup>) and *Gr8a* mutant *D. melanogaster* males with oenocyte-specific *D. mojavensis Gr8a* rescue (*Gr8a*; *desat1* > *Gr8a*<sup>*mojavensis*</sup>). Alkanes denoted as C<sub>n</sub>, where n denotes the number of carbon atoms in the chain. Alkenes denoted as N-C<sub>n</sub>, where N denotes the location of carbon-carbon double bond in chain. Methyl-branched alkanes denoted as NMe-C<sub>n</sub>, where N denotes the carbon in the chain at which the methyl branch occurs. See [Data S1](#) "P-value data" for exact p values.

linkage in signal-receptor pairs important for mating communication is likely to be more common than previously thought. Therefore, the genetic tractability of *D. melanogaster*, in combination with the diversity of mating communication systems in this species-rich phylogenetic group, provide a unique opportunity for understanding the evolution and mechanisms that drive and maintain the robustness of mating systems at the genetic, molecular, and cellular levels.

### Limitations of the study

The present study provides evidence that *Gr8a* plays a role in both the production and detection of mating pheromones in *D. melanogaster*. We base our conclusion that *Gr8a*-expressing GRNs detect mating pheromones on our behavioral studies, which suggest that *Gr8a* mutations affect male and female responses to

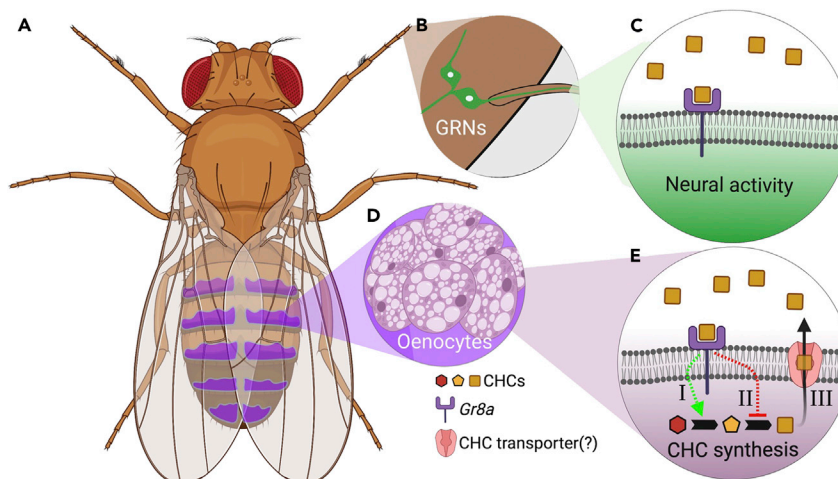


**Figure 7. Model for the pleiotropic action of *Gr8a* in the perception and production of pheromones**

- (A) *Drosophila* male. The location of CHC-producing oenocytes is shown in magenta.  
 (B) *Gr8a*-expressing GRNs are located at the last tarsal segment of the prothoracic legs.  
 (C) *Gr8a* functions as an inhibitory pheromone receptor in a specific subset of leg GRNs.  
 (D) Oenocytes are the primary CHC-producing cells in the male abdomen.  
 (E) *Gr8a* functions as an autoreceptor in oenocytes, which regulates CHC synthesis [I-II] and/or CHC secretion [III] via signaling feedback loops.

an inhibitory mating signal. While these findings are consistent with a role for *Gr8a* in sensory detection, our study does not use functional approaches that directly assess the responsiveness of *Gr8a*-expressing GRNs to cuticular pheromones. Such approaches, including electrophysiology and functional imaging, can be incorporated into future work on *Gr8a*-expressing GRNs to establish this link at the functional level.

## STAR★METHODS

Detailed methods are provided in the online version of this paper and include the following:

- KEY RESOURCES TABLE
- RESOURCE AVAILABILITY
  - Lead contact
  - Materials availability
  - Data and code availability
- EXPERIMENTAL MODEL AND SUBJECT DETAILS
- METHOD DETAILS
  - Immunohistochemistry
  - mRNA expression
  - Courtship behavior assays
  - Perfuming studies
  - Phylogenetic analysis
  - Pheromone analysis
- QUANTIFICATION AND STATISTICAL ANALYSIS

## SUPPLEMENTAL INFORMATION

Supplemental information can be found online at <https://doi.org/10.1016/j.isci.2022.105882>.

## ACKNOWLEDGMENTS

We thank members of the Ben-Shahar lab for their comments on earlier versions of the article. We thank Joshua Krupp (University of Toronto) for assistance with perfuming studies, Nabeel Chowdhury and Deanna Simon for assistance with qRT-PCR analysis, and Paula Kiefel for technical help with generating transgenic flies. This work was supported by NSF grants 1322783, 1754264, and 1707221, and NIH grant NS089834 awarded to Y. B-S. Stocks obtained from the Bloomington *Drosophila* Stock Center (NIH

P40OD018537) were used in this study. Wild-type *Drosophila* species were obtained from the National *Drosophila* Species Stock Center at Cornell University.

### AUTHOR CONTRIBUTIONS

C.L.V., N.L., K.M.Z., J.G.M., and Y.B-S designed experiments. C.L.V., N.L., K.M.Z., S.D., M.F., X.L., S.H., J.G.M., and Y.B-S collected and analyzed data. C.L.V., N.L., K.M.Z., and Y.B-S wrote the article.

### DECLARATION OF INTERESTS

The authors declare no competing interests.

### INCLUSION AND DIVERSITY

We support inclusive, diverse, and equitable conduct of research.

Received: January 17, 2022

Revised: November 17, 2022

Accepted: December 21, 2022

Published: January 20, 2023

### REFERENCES

- Boake, C.R. (1991). Coevolution of senders and receivers of sexual signals: genetic coupling and genetic correlations. *Trends Ecol. Evol.* 6, 225–227. [https://doi.org/10.1016/0169-5347\(91\)90027-U](https://doi.org/10.1016/0169-5347(91)90027-U).
- Brooks, R., Hunt, J., Blows, M.W., Smith, M.J., Bussière, L.F., and Jennions, M.D. (2005). Experimental evidence for multivariate stabilizing sexual selection. *Evolution* 59, 871–880. <https://doi.org/10.1111/j.0014-3820.2005.tb01760.x>.
- Hoy, R.R., Hahn, J., and Paul, R.C. (1977). Hybrid cricket auditory behavior: evidence for genetic coupling in animal communication. *Science* 195, 82–84. <https://doi.org/10.1126/science.831260>.
- Singh, N.D., and Shaw, K.L. (2012). On the scent of pleiotropy. *Proc. Natl. Acad. Sci. USA* 109, 5–6. <https://doi.org/10.1073/pnas.1118531109>.
- Shaw, K.L., and Lesnick, S.C. (2009). Genomic linkage of male song and female acoustic preference QTL underlying a rapid species radiation. *Proc. Natl. Acad. Sci. USA* 106, 9737–9742. <https://doi.org/10.1073/pnas.0900229106>.
- Steiger, S., Schmitt, T., and Schaefer, H.M. (2011). The origin and dynamic evolution of chemical information transfer. *Proc. Biol. Sci.* 278, 970–979. <https://doi.org/10.1098/rspb.2010.2285>.
- Sweigart, A.L. (2010). The genetics of postmating, prezygotic reproductive isolation between *Drosophila virilis* and *D. americana*. *Genetics* 184, 401–410. <https://doi.org/10.1534/genetics.109.111245>.
- Symonds, M.R.E., and Elgar, M.A. (2008). The evolution of pheromone diversity. *Trends Ecol. Evol.* 23, 220–228. <https://doi.org/10.1016/j.tree.2007.11.009>.
- Wyatt, T.D. (2014). *Pheromones and Animal Behavior: Chemical Signals and Signatures*, 2nd edition (Cambridge University Press).
- Butlin, R.K., and Ritchie, M.G. (1989). Genetic coupling in mate recognition systems: what is the evidence? *Biol. J. Linn. Soc.* 37, 237–246. <https://doi.org/10.1111/j.1095-8312.1989.tb01902.x>.
- Butlin, R.K., and Trickett, A.J. (1997). Can population genetic simulations help to 734 interpret pheromone evolution? In *Insect Pheromone Research*, R.T. Cardé and A.K. Minks, eds. (Chapman and Hall), pp. 548–562.
- Shaw, K.L., Ellison, C.K., Oh, K.P., and Wiley, C. (2011). Pleiotropy, “sexy” traits, and speciation. *Behav. Ecol.* 22, 1154–1155. <https://doi.org/10.1093/beheco/arr136>.
- Chebib, J., and Guillaume, F. (2021). Pleiotropy or linkage? Their relative contributions to the genetic correlation of quantitative traits and detection by multitrait GWA studies. *Genetics* 219, iyab159. <https://doi.org/10.1093/genetics/iyab159>.
- Kirkpatrick, M., and Hall, D.W. (2004). Sexual selection and sex linkage. *Evolution* 58, 683–691.
- Lande, R. (1980). The genetic covariance between characters maintained by pleiotropic mutations. *Genetics* 94, 203–215.
- Wiley, C., Ellison, C.K., and Shaw, K.L. (2012). Widespread genetic linkage of mating signals and preferences in the Hawaiian cricket *Laupala*. *Proc. Biol. Sci.* 279, 1203–1209. <https://doi.org/10.1098/rspb.2011.1740>.
- Chenoweth, S.F., and Blows, M.W. (2006). Dissecting the complex genetic basis of mate choice. *Nat. Rev. Genet.* 7, 681–692. <https://doi.org/10.1038/nrg1924>.
- Chung, H., and Carroll, S.B. (2015). Wax, sex and the origin of species: dual roles of insect cuticular hydrocarbons in adaptation and mating. *Bioessays* 37, 822–830. <https://doi.org/10.1002/bies.201500014>.
- Chung, H., Loehlin, D.W., Dufour, H.D., Vaccarro, K., Millar, J.G., and Carroll, S.B. (2014). A single gene affects both ecological divergence and mate choice in *Drosophila*. *Science* 343, 1148–1151.
- McKinney, R.M., Vernier, C., and Ben-Shahar, Y. (2015). The neural basis for insect pheromonal communication. *Curr. Opin. Insect Sci.* 12, 86–92. <https://doi.org/10.1016/j.cois.2015.09.010>.
- Bousquet, F., Nojima, T., Houot, B., Chauvel, I., Chaudy, S., Dupas, S., Yamamoto, D., and Ferveur, J.-F. (2012). Expression of a desaturase gene, *desat1*, in neural and nonneural tissues separately affects perception and emission of sex pheromones in *Drosophila*. *Proc. Natl. Acad. Sci. USA* 109, 249–254. <https://doi.org/10.1073/pnas.1109166108>.
- Lee, Y., Kang, M.J., Shim, J., Cheong, C.U., Moon, S.J., and Montell, C. (2012). Gustatory receptors required for avoiding the insecticide L-canavanine. *J. Neurosci.* 32, 1429–1435. <https://doi.org/10.1523/JNEUROSCI.4630-11.2012>.
- Shim, J., Lee, Y., Jeong, Y.T., Kim, Y., Lee, M.G., Montell, C., and Moon, S.J. (2015). The full repertoire of *Drosophila* gustatory receptors for detecting an aversive compound. *Nat. Commun.* 6, 8867. <https://doi.org/10.1038/ncomms9867>.
- Billeter, J.C., Atallah, J., Krupp, J.J., Millar, J.G., and Levine, J.D. (2009). Specialized cells tag sexual and species identity in *Drosophila melanogaster*. *Nature* 461, 987–991. <https://doi.org/10.1038/nature08495>.
- Gutierrez, E., Wiggins, D., Fielding, B., and Gould, A.P. (2007). Specialized hepatocyte-like cells regulate *Drosophila* lipid metabolism. *Nature* 445, 275–280. <https://doi.org/10.1038/nature05382>.
- Blomquist, G.J., and Bagnères, A.-G. (2010). *Insect Hydrocarbons: Biology, Biochemistry*,

- and Chemical Ecology (Cambridge University Press).
27. Ferveur, J.F. (2005). Cuticular hydrocarbons: their evolution and roles in *Drosophila* pheromonal communication. *Behav. Genet.* 35, 279–295. <https://doi.org/10.1007/s10519-005-3220-5>.
  28. Ben-Shahar, Y. (2015). Editorial overview: neuroscience: How nervous systems generate behavior: lessons from insects. *Curr. Opin. Insect Sci.* 12, v–vii. <https://doi.org/10.1016/j.cois.2015.10.005>.
  29. Dweck, H.K.M., Ebrahim, S.A.M., Thoma, M., Mohamed, A.A.M., Keesey, I.W., Trona, F., Lavista-Llanos, S., Svatoš, A., Sachse, S., Knaden, M., et al. (2015). Pheromones mediating copulation and attraction in *Drosophila*. *Proc. Natl. Acad. Sci. USA* 112, E2829–E2835. <https://doi.org/10.1073/pnas.1504527112>.
  30. Lu, B., Zelle, K.M., Seltzer, R., Hefetz, A., and Ben-Shahar, Y. (2014). Feminization of pheromone-sensing neurons affects mating decisions in *Drosophila* males. *Biol. Open* 3, 152–160. <https://doi.org/10.1242/bio.20147369>.
  31. Lu, B., LaMora, A., Sun, Y., Welsh, M.J., and Ben-Shahar, Y. (2012). ppk23-Dependent chemosensory functions contribute to courtship behavior in *Drosophila melanogaster*. *PLoS Genet.* 8, e1002587. <https://doi.org/10.1371/journal.pgen.1002587>.
  32. Yew, J.Y., and Chung, H. (2015). Insect pheromones: an overview of function, form, and discovery. *Prog. Lipid Res.* 59, 88–105. <https://doi.org/10.1016/j.plipres.2015.06.001>.
  33. Howard, R.W., and Blomquist, G.J. (2005). Ecological, behavioral, and biochemical aspects of insect hydrocarbons. *Annu. Rev. Entomol.* 50, 371–393. <https://doi.org/10.1146/annurev.ento.50.071803.130359>.
  34. Benton, R., Vannice, K.S., and Vosshall, L.B. (2007). An essential role for a CD36-related receptor in pheromone detection in *Drosophila*. *Nature* 450, 289–293. <https://doi.org/10.1038/nature06328>.
  35. Clowney, E.J., Iguchi, S., Bussell, J.J., Scheer, E., and Ruta, V. (2015). Multimodal chemosensory circuits controlling male courtship in *Drosophila*. *Neuron* 87, 1036–1049. <https://doi.org/10.1016/j.neuron.2015.07.025>.
  36. Datta, S.R., Vasconcelos, M.L., Ruta, V., Luo, S., Wong, A., Demir, E., Flores, J., Balonze, K., Dickson, B.J., and Axel, R. (2008). The *Drosophila* pheromone cVA activates a sexually dimorphic neural circuit. *Nature* 452, 473–477. <https://doi.org/10.1038/nature06808>.
  37. Koh, T.W., He, Z., Gorur-shandilya, S., Menuz, K., Larter, N.K., Stewart, S., and Carlson, J.R. (2014). The *Drosophila* IR20a clade of ionotropic receptors are candidate taste and pheromone receptors. *Neuron* 83, 850–865. <https://doi.org/10.1016/j.neuron.2014.07.012>.
  38. Kurtovic, A., Widmer, A., and Dickson, B.J. (2007). A single class of olfactory neurons mediates behavioural responses to a *Drosophila* sex pheromone. *Nature* 446, 542–546. <https://doi.org/10.1038/nature05672>.
  39. Lebreton, S., Grabe, V., Omondi, A.B., Ignell, R., Becher, P.G., Hansson, B.S., Sachse, S., and Witzgall, P. (2014). Love makes smell blind: mating suppresses pheromone attraction in *Drosophila* females via Or65a olfactory neurons. *Sci. Rep.* 4, 7119. <https://doi.org/10.1038/srep07119>.
  40. Pikielny, C.W. (2012). Sexy DEG/ENaC channels involved in gustatory detection of fruit fly pheromones. *Sci. Signal.* 5, pe48. <https://doi.org/10.1126/scisignal.2003555>.
  41. Thistle, R., Cameron, P., Ghorayshi, A., Dennison, L., and Scott, K. (2012). Contact chemoreceptors mediate male-male repulsion and male-female attraction during *Drosophila* courtship. *Cell* 149, 1140–1151. <https://doi.org/10.1016/j.cell.2012.03.045>.
  42. Toda, H., Zhao, X., and Dickson, B.J. (2012). The *Drosophila* female aphrodisiac pheromone activates ppk23+ sensory neurons to elicit male courtship behavior. *Cell Rep.* 1, 599–607. <https://doi.org/10.1016/j.celrep.2012.05.007>.
  43. van der Goes van Naters, W., and Carlson, J.R. (2007). Receptors and neurons for fly odors in *Drosophila*. *Curr. Biol.* 17, 606–612. <https://doi.org/10.1016/j.cub.2007.02.043>.
  44. Bray, S., and Amrein, H. (2003). A putative *Drosophila* pheromone receptor expressed in male-specific taste neurons is required for efficient courtship. *Neuron* 39, 1019–1029. [https://doi.org/10.1016/S0896-6273\(03\)00542-7](https://doi.org/10.1016/S0896-6273(03)00542-7).
  45. Miyamoto, T., and Amrein, H. (2008). Suppression of male courtship by a *Drosophila* pheromone receptor. *Nat. Neurosci.* 11, 874–876. <https://doi.org/10.1038/nn.2161>.
  46. Moon, S.J., Lee, Y., Jiao, Y., and Montell, C. (2009). A *Drosophila* gustatory receptor essential for aversive taste and inhibiting male-to-male courtship. *Curr. Biol.* 19, 1623–1627. <https://doi.org/10.1038/jid.2014.371>.
  47. Watanabe, K., Toba, G., Koganezawa, M., and Yamamoto, D. (2011). Gr39a, a highly diversified gustatory receptor in *Drosophila*, has a role in sexual behavior. *Behav. Genet.* 41, 746–753. <https://doi.org/10.1007/s10519-011-9461-6>.
  48. Clyne, P.J., Warr, C.G., and Carlson, J.R. (2000). Candidate taste receptors in *Drosophila*. *Science* 287, 1830–1834. <https://doi.org/10.1126/science.287.5459.1830>.
  49. Dunipace, L., Meister, S., Mcnealy, C., and Amrein, H. (2001). Spatially restricted expression of candidate taste receptors in the. *Curr. Biol.* 11, 822–835.
  50. Scott, K., Brady, R., Cravchik, A., Morozov, P., Rzhetsky, A., Zuker, C., and Axel, R. (2001). A chemosensory gene family encoding candidate gustatory and olfactory receptors in *Drosophila*. *Cell* 104, 661–673. [https://doi.org/10.1016/S0092-8674\(01\)00263-X](https://doi.org/10.1016/S0092-8674(01)00263-X).
  51. Wang, Z., Singhvi, A., Kong, P., and Scott, K. (2004). Taste representations in the *Drosophila* brain. *Cell* 117, 981–991. <https://doi.org/10.1016/j.cell.2004.06.011>.
  52. Lacaille, F., Hiroi, M., Twele, R., Inoshita, T., Umemoto, D., Manière, G., Marion-Poll, F., Ozaki, M., Francke, W., Cobb, M., et al. (2007). An inhibitory sex pheromone tastes bitter for *Drosophila* males. *PLoS One* 2, e661. <https://doi.org/10.1371/journal.pone.0000661>.
  53. Park, J.H., and Kwon, J.Y. (2011). A systematic analysis of *Drosophila* gustatory receptor gene expression in abdominal neurons which project to the central nervous system. *Mol. Cell.* 32, 375–381. <https://doi.org/10.1007/s10059-011-0128-1>.
  54. Hu, Y., Tattikota, S.G., Liu, Y., Comjean, A., Gao, Y., Forman, C., Kim, G., Rodiger, J., Papatheodorou, I., dos Santos, G., et al. (2021). DRscDB: a single-cell RNA-seq resource for data mining and data comparison across species. *Comput. Struct. Biotechnol. J.* 19, 2018–2026. <https://doi.org/10.1016/j.csbj.2021.04.021>.
  55. Ling, F., Dahanukar, A., Weiss, L.A., Kwon, J.Y., and Carlson, J.R. (2014). The molecular and cellular basis of taste coding in the legs of *Drosophila*. *J. Neurosci.* 34, 7148–7164. <https://doi.org/10.1523/JNEUROSCI.0649-14.2014>.
  56. Ejima, A., Smith, B.P.C., Lucas, C., van der Goes van Naters, W., Miller, C.J., Carlson, J.R., Levine, J.D., and Griffith, L.C. (2007). Generalization of courtship learning in *Drosophila* is mediated by cis-vaccenyl acetate. *Curr. Biol.* 17, 599–605. <https://doi.org/10.1016/j.cub.2007.01.053>.
  57. Yew, J.Y., Dreisewerd, K., Luftmann, H., Müthing, J., Pohlentz, G., and Kravitz, E.A. (2009). A new male sex pheromone and novel cuticular cues for chemical communication in *Drosophila*. *Curr. Biol.* 19, 1245–1254. <https://doi.org/10.1016/j.cub.2009.06.037>.
  58. Jallon, J.-M. (1984). A few chemical words exchanged by *Drosophila* during courtship and mating. *Behav. Genet.* 14, 441–478.
  59. Averhoff, W.W., and Richardson, R.H. (1974). Pheromonal control of mating patterns in *Drosophila melanogaster*. *Behav. Genet.* 4, 207–225. <https://doi.org/10.1007/BF01074155>.
  60. Jin, X., Ha, T.S., and Smith, D.P. (2008). SNMP is a signaling component required for pheromone sensitivity in *Drosophila*. *Proc. Natl. Acad. Sci. USA* 105, 10996–11001. <https://doi.org/10.1073/pnas.0803309105>.
  61. Yang, C.H., Rumpf, S., Xiang, Y., Gordon, M.D., Song, W., Jan, L.Y., and Jan, Y.N. (2009). Control of the postmating behavioral switch in *Drosophila* females by internal sensory neurons. *Neuron* 61, 519–526. <https://doi.org/10.1016/j.neuron.2008.12.021>.
  62. Ugrankar, R., Bowerman, J., Hariri, H., Chandra, M., Chen, K., Bossanyi, M.F., Datta, S., Rogers, S., Eckert, K.M., Vale, G., et al.

- (2019). *Drosophila snazarus* regulates a lipid droplet population at plasma membrane-droplet contacts in adipocytes. *Dev. Cell* 50, 557–572.e5. <https://doi.org/10.1016/j.devcel.2019.07.021>.
63. Sweeney, S.T., Broadie, K., Keane, J., Niemann, H., and O’kane, C.J. (1995). Targeted expression of tetanus toxin light chain in *Drosophila* specifically eliminates synaptic transmission and causes behavioral defects. *Neuron* 14, 341–351.
64. Kallman, B.R., Kim, H., and Scott, K. (2015). Excitation and inhibition onto central courtship neurons biases *Drosophila* mate choice. *Elife* 4, e11188. <https://doi.org/10.7554/eLife.11188>.
65. Krupp, J.J., Kent, C., Billeter, J.C., Azanchi, R., So, A.K.C., Schonfeld, J.A., Smith, B.P., Lucas, C., and Levine, J.D. (2008). Social experience modifies pheromone expression and mating behavior in male *Drosophila melanogaster*. *Curr. Biol.* 18, 1373–1383. <https://doi.org/10.1016/j.cub.2008.07.089>.
66. Laturney, M., and Billeter, J.C. (2016). *Drosophila melanogaster* females restore their attractiveness after mating by removing male anti-aphrodisiac pheromones. *Nat. Commun.* 7, 12322. <https://doi.org/10.1038/ncomms12322>.
67. Siwicki, K.K., Riccio, P., Ladewski, L., Marcillac, F., Darteville, L., Cross, S.A., and Ferveur, J.F. (2005). The role of cuticular pheromones in courtship conditioning of *Drosophila* males. *Learn. Mem.* 12, 636–645. <https://doi.org/10.1101/lm.85605>.
68. Krupp, J.J., Billeter, J.C., Wong, A., Choi, C., Nitabach, M.N., and Levine, J.D. (2013). Pigment-dispersing factor modulates pheromone production in clock cells that influence mating in *Drosophila*. *Neuron* 79, 54–68. <https://doi.org/10.1016/j.neuron.2013.05.019>.
69. Sureau, G., and Ferveur, J.F. (1999). Co-adaptation of pheromone production and behavioural responses in *Drosophila melanogaster* males. *Genet. Res.* 74, 129–137. <https://doi.org/10.1017/S0016672399003936>.
70. Ben-Shahar, Y., Lu, B., Collier, D.M., Snyder, P.M., Schnizler, M., and Welsh, M.J. (2010). The *Drosophila* gene *CheB42a* is a novel modifier of *Deg/ENaC* channel function. *PLoS One* 5, e9395. <https://doi.org/10.1371/journal.pone.0009395>.
71. Ben-Shahar, Y., Nannapaneni, K., Casavant, T.L., Scheetz, T.E., and Welsh, M.J. (2007). Eukaryotic operon-like transcription of functionally related genes in *Drosophila*. *Proc. Natl. Acad. Sci. USA* 104, 222–227. <https://doi.org/10.1073/pnas.0609683104>.
72. Leitner, N., and Ben-Shahar, Y. (2020). The neurogenetics of sexually dimorphic behaviors from a postdevelopmental perspective. *Genes Brain Behav.* 19, e12623. <https://doi.org/10.1111/gbb.12623>.
73. Khallaf, M.A., Cui, R., Weißflog, J., Erdogmus, M., Svatoš, A., Dweck, H.K.M., Valenzano, D.R., Hansson, B.S., and Knaden, M. (2021). Large-scale characterization of sex pheromone communication systems in *Drosophila*. *Nat. Commun.* 12, 4165. <https://doi.org/10.1038/s41467-021-24395-z>.
74. Symonds, M.R.E., and Wertheim, B. (2005). The mode of evolution of aggregation pheromones in *Drosophila* species. *J. Evol. Biol.* 18, 1253–1263. <https://doi.org/10.1111/j.1420-9101.2005.00971.x>.
75. Shahandeh, M.P., Pischedda, A., and Turner, T.L. (2018). Male mate choice via cuticular hydrocarbon pheromones drives reproductive isolation between *Drosophila* species. *Evolution* 72, 123–135. <https://doi.org/10.1111/evo.13389>.
76. Shirangi, T.R., Dufour, H.D., Williams, T.M., and Carroll, S.B. (2009). Rapid evolution of sex pheromone-producing enzyme expression in *Drosophila*. *PLoS Biol.* 7, e1000168. <https://doi.org/10.1371/journal.pbio.1000168>.
77. Ford, C.P. (2014). The role of D2-autoreceptors in regulating dopamine neuron activity and transmission. *Neuroscience* 282, 13–22. <https://doi.org/10.1016/j.neuroscience.2014.01.025>.
78. Stagkourakis, S., Kim, H., Lyons, D.J., and Broberger, C. (2016). Dopamine autoreceptor regulation of a hypothalamic dopaminergic network. *Cell Rep.* 15, 735–747. <https://doi.org/10.1016/j.celrep.2016.03.062>.
79. Dweck, H.K.M., and Carlson, J.R. (2020). Molecular logic and evolution of bitter taste in *Drosophila*. *Curr. Biol.* 30, 17–30.e3. <https://doi.org/10.1016/j.cub.2019.11.005>.
80. Sung, H.Y., Jeong, Y.T., Lim, J.Y., Kim, H., Oh, S.M., Hwang, S.W., Kwon, J.Y., and Moon, S.J. (2017). Heterogeneity in the *Drosophila* gustatory receptor complexes that detect aversive compounds. *Nat. Commun.* 8, 1484. <https://doi.org/10.1038/s41467-017-01639-5>.
81. Lee, Y., Moon, S.J., and Montell, C. (2009). Multiple gustatory receptors required for the caffeine response in *Drosophila*. *Proc. Natl. Acad. Sci. USA* 106, 4495–4500. <https://doi.org/10.1073/pnas.0811744106>.
82. Poudel, S., Kim, Y., Kim, Y.T., and Lee, Y. (2015). Gustatory receptors required for sensing umbelliferone in *Drosophila melanogaster*. *Insect Biochem. Mol. Biol.* 66, 110–118. <https://doi.org/10.1016/j.ibmb.2015.10.010>.
83. Shankar, S., Chua, J.Y., Tan, K.J., Calvert, M.E.K., Weng, R., Ng, W.C., Mori, K., and Yew, J.Y. (2015). The neuropeptide tachykinin is essential for pheromone detection in a gustatory neural circuit. *Elife* 4, e06914. <https://doi.org/10.7554/eLife.06914>.
84. Heinen-Kay, J.L., Nichols, R.E., and Zuk, M. (2020). Sexual signal loss, pleiotropy, and maintenance of a male reproductive polymorphism in crickets. *Evolution* 74, 1002–1009. <https://doi.org/10.1111/evo.13952>.
85. Fukamachi, S., Kinoshita, M., Aizawa, K., Oda, S., Meyer, A., and Mitani, H. (2009). Dual control by a single gene of secondary sexual characters and mating preferences in medaka. *BMC Biol.* 7, 64. <https://doi.org/10.1186/1741-7007-7-64>.
86. Abascal, F., Zardoya, R., and Posada, D. (2005). ProtTest: selection of best-fit models of protein evolution. *Bioinformatics* 21, 2104–2105. <https://doi.org/10.1093/bioinformatics/bti263>.
87. Sievers, F., Wilm, A., Dineen, D., Gibson, T.J., Karplus, K., Li, W., Lopez, R., McWilliam, H., Remmert, M., Söding, J., et al. (2011). Fast, scalable generation of high-quality protein multiple sequence alignments using Clustal Omega. *Mol. Syst. Biol.* 7, 539. <https://doi.org/10.1038/msb.2011.75>.
88. Zheng, X., Valakh, V., DiAntonio, A., and Ben-Shahar, Y. (2014). Natural antisense transcripts regulate the neuronal stress response and excitability. *Elife* 3, e01849. <https://doi.org/10.7554/eLife.01849>.
89. Pfeiffer, B.D., Ngo, T.T.B., Hibbard, K.L., Murphy, C., Jenett, A., Truman, J.W., and Rubin, G.M. (2010). Refinement of tools for targeted gene expression in *Drosophila*. *Genetics* 186, 735–755. <https://doi.org/10.1534/genetics.110.119917>.
90. Hill, A., Zheng, X., Li, X., McKinney, R., Dickman, D., and Ben-Shahar, Y. (2017). The *Drosophila* postsynaptic *DEG/ENaC* channel *ppk29* contributes to excitatory neurotransmission. *J. Neurosci.* 37, 3171–3180. <https://doi.org/10.1523/jneurosci.3850-16.2017>.
91. Hill, A.S., Jain, P., Folan, N.E., and Ben-Shahar, Y. (2019). The *Drosophila* ERG channel seizure plays a role in the neuronal homeostatic stress response. *PLoS Genet.* 15, e1008288. <https://doi.org/10.1371/journal.pgen.1008288>.
92. Miller, M., Pfeiffer, W.T., and Schwartz, T. (2010). Creating the CIPRES science gateway for inference of large phylogenetic trees. In 2010 Gateway Computing Environments Workshop (GCE). <https://doi.org/10.1109/GCE.2010.5676129>.
93. R Core Team. R: A language and environment for statistical computing. 2013; 201.
94. Pohlert, T. (2014). The Pairwise Multiple Comparison of Mean Ranks Package (PMCMR). R Package 7, 10.
95. Oksanen, J., Blanchet, F.G., Friendly, M., Kindt, R., Legendre, P., McGinn, D., et al. (2013). Community ecology package. R package version 2.0, 321–326.



## STAR★METHODS

### KEY RESOURCES TABLE

REAGENT or RESOURCE	SOURCE	IDENTIFIER
<b>Antibodies</b>		
Rabbit GFP Polyclonal Antibody	ThermoFisher Scientific	Cat#A-11122; RRID: AB_221569
Mouse Firefly luciferase Monoclonal Antibody	ThermoFisher Scientific	Cat#35-6700; RRID: AB_2533218
Donkey anti-Rabbit Secondary Antibody, Alexa Fluor 488	ThermoFisher Scientific	Cat#A-21206; RRID: AB_2535792
Donkey anti-Mouse Secondary Antibody, Alexa Fluor 568	ThermoFisher Scientific	Cat#A-10037; RRID: AB_2534013
<b>Bacterial and virus strains</b>		
NEB 5-alpha Competent <i>E. coli</i>	New England BioLabs	Cat#C29871
<b>Chemicals, peptides, and recombinant proteins</b>		
Hexane	Sigma-Aldrich	Cat#139386
Hexacosane (C <sub>26</sub> )	Sigma-Aldrich	Cat#241687
9-C <sub>25</sub>	This paper, Millar Lab	N/A
7-C <sub>25</sub>	This paper, Millar Lab	N/A
5-C <sub>25</sub>	This paper, Millar Lab	N/A
7-C <sub>27</sub>	This paper, Millar Lab	N/A
Pentacosane (C <sub>25</sub> )	Sigma-Aldrich	Cat#76493
Heptacosane (C <sub>27</sub> )	Sigma-Aldrich	Cat#51559
Nonacosane (C <sub>29</sub> )	Sigma-Aldrich	Cat#74156
TRIZOL Reagent	ThermoFisher Scientific	Cat#15596018
Super-Script II reverse transcriptase	ThermoFisher Scientific	Cat#18064022
<b>Deposited data</b>		
Raw data	This paper	Mendeley Data: <a href="https://doi.org/10.17632/y5gnn6stpj.2">https://doi.org/10.17632/y5gnn6stpj.2</a>
<b>Experimental models: Organisms/strains</b>		
<i>D. melanogaster</i> : P{UAS-TeTxLC.tnt}E2	Bloomington Drosophila Stock Center	BDSC: 28837 FlyBase: FBti0038528
<i>D. melanogaster</i> : P{UAS-TeTxLC.(-)V}	Bloomington Drosophila Stock Center	BDSC: 28840 FlyBase: FBtp0001266
<i>D. melanogaster</i> : w <sup>*</sup> ; P{10XUAS-IVS-mCD8::GFP}attP40	Bloomington Drosophila Stock Center	BDSC: 32186 FlyBase: FBst0032186
<i>D. melanogaster</i> : w <sup>*</sup> ; P{13XLexAop2-IVS-myr::GFP}attP40	Bloomington Drosophila Stock Center	BDSC: 32210 FlyBase: FBst0032210
<i>D. melanogaster</i> : w <sup>*</sup> ; P{UAS-RedStinger}6, P{UAS-FLP.Exel}3, P{Ubi-p63E(FRT.STOP)Stinger}15F2	Bloomington Drosophila Stock Center	BDSC: 28281 FlyBase: FBst0028281
<i>D. melanogaster</i> : Df(1)BSC663, w <sup>1118</sup> /FM7h/Dp(2; Y)G, P{hs-hid}Y	Bloomington Drosophila Stock Center	BDSC: 26515 FlyBase: FBab0045733
<i>D. melanogaster</i> : Df(1)BSC754, w <sup>1118</sup> /Binsincy	Bloomington Drosophila Stock Center	BDSC: 26852 FlyBase: FBab0045821
<i>D. melanogaster</i> : w <sup>*</sup> ; P{Gr8a-GAL4.0.7}5/CyO; Dr <sup>1</sup> /TM3, Sb <sup>1</sup>	Bloomington Drosophila Stock Center	BDSC: 57594 FlyBase: FBst0057594
<i>D. melanogaster</i> : w <sup>*</sup> Gr8a <sup>1</sup>	Bloomington Drosophila Stock Center	BDSC: 40976 FlyBase: FBst0040976

(Continued on next page)

**Continued**

REAGENT or RESOURCE	SOURCE	IDENTIFIER
<i>D. melanogaster</i> : w <sup>*</sup> ; P[Desat1-GAL4.E800]2M/CyO	Bloomington Drosophila Stock Center	BDSC: 65404 FlyBase: FBst0065404
<i>D. melanogaster</i> : y <sup>1</sup> w <sup>*</sup> ; P{r4-GAL4}3	Bloomington Drosophila Stock Center	BDSC: 33832 FlyBase: FBst0033832
<i>D. melanogaster</i> : w <sup>*</sup> ; wg <sup>SP-1</sup> /CyO; Tl{lexA::VP16}fru <sup>P1.LexA</sup> /TM6B, Tb <sup>1</sup>	Bloomington Drosophila Stock Center	BDSC: 66698 FlyBase: FBti0168676
<i>D. melanogaster</i> : w <sup>*</sup> ; P[Desat1-GAL4.E800]4M	Levine Lab, Bloomington Drosophila Stock Center	BDSC: 65405 FlyBase: FBst0065405
<i>D. melanogaster</i> : PromE(800)>Luciferase	Levine Lab	N/A
<i>D. melanogaster</i> : Gr8a <sup>1</sup> ; UAS-Gr8a <sub>mojavensis</sub> /cyo	This paper, Ben-Shahar Lab	N/A
<i>D. melanogaster</i> : Gr8a <sup>1</sup> ; UAS-Gr8a <sub>melanogaster</sub> /cyo	This paper, Ben-Shahar Lab	N/A
<i>D. melanogaster</i> : ppk23-LexA, LexAop-GFP/cyo; UAS-Red-Stinger/tm3	This paper, Ben-Shahar Lab	N/A
<i>D. melanogaster</i> : Gr8a CRISPR GFP tagged/FM7gfp	This paper, Ben-Shahar Lab	N/A
<i>D. simulans</i>	National Drosophila Species Stock Center	<a href="https://www.drosophilaspecies.com/shop/simulans/">https://www.drosophilaspecies.com/shop/simulans/</a>
<i>D. sechellia</i>	National Drosophila Species Stock Center	<a href="https://www.drosophilaspecies.com/shop/d-sechellia/">https://www.drosophilaspecies.com/shop/d-sechellia/</a>
<i>D. yakuba</i>	National Drosophila Species Stock Center	<a href="https://www.drosophilaspecies.com/shop/yakuba/">https://www.drosophilaspecies.com/shop/yakuba/</a>
<i>D. erecta</i>	National Drosophila Species Stock Center	<a href="https://www.drosophilaspecies.com/shop/d-erecta/">https://www.drosophilaspecies.com/shop/d-erecta/</a>
<i>D. ananassae</i>	National Drosophila Species Stock Center	<a href="https://www.drosophilaspecies.com/shop/ananassae/">https://www.drosophilaspecies.com/shop/ananassae/</a>
<i>D. pseudoobscura</i>	National Drosophila Species Stock Center	<a href="https://www.drosophilaspecies.com/shop/d-pseudoobscura/">https://www.drosophilaspecies.com/shop/d-pseudoobscura/</a>
<i>D. persimilis</i>	National Drosophila Species Stock Center	<a href="https://www.drosophilaspecies.com/shop/d-persimilis/">https://www.drosophilaspecies.com/shop/d-persimilis/</a>
<i>D. willistoni</i>	National Drosophila Species Stock Center	<a href="https://www.drosophilaspecies.com/shop/d-willistoni/">https://www.drosophilaspecies.com/shop/d-willistoni/</a>
<i>D. mojavensis</i>	National Drosophila Species Stock Center	<a href="https://www.drosophilaspecies.com/shop/d-mojavensis/">https://www.drosophilaspecies.com/shop/d-mojavensis/</a>
<i>D. virilis</i>	National Drosophila Species Stock Center	<a href="https://www.drosophilaspecies.com/shop/d-virilis/">https://www.drosophilaspecies.com/shop/d-virilis/</a>
<b>Oligonucleotides</b>		
RT-PCR primers for <i>D. melanogaster</i> GR genes	This paper	Table S1
qRT-PCR primers for <i>D. melanogaster</i> Gr8a and Rp49 and orthologs	This paper	Table S2
qRT-PCR primers for <i>D. melanogaster</i> desaturase enzyme genes	This paper	Table S3
<b>Recombinant DNA</b>		
Plasmid: GFP tagged Gr8a	This paper, Ben-Shahar Lab	N/A
Plasmid: UAS-Gr8a <sub>mojavensis</sub>	This paper, Ben-Shahar Lab	N/A
Plasmid: UAS-Gr8a <sub>melanogaster</sub>	This paper, Ben-Shahar Lab	N/A
Plasmid: ppk23-LexA	This paper, Ben-Shahar Lab	N/A

(Continued on next page)

**Continued**

REAGENT or RESOURCE	SOURCE	IDENTIFIER
<b>Software and algorithms</b>		
R v4.2.0	R core team <sup>86</sup>	<a href="https://www.R-project.org/">https://www.R-project.org/</a>
CIPRES	Miller et al. <sup>87</sup>	<a href="https://www.phylo.org">https://www.phylo.org</a>
DRscDB	Hu et al. <sup>54</sup>	<a href="https://www.flymai.org/tools/single_cell/web/">https://www.flymai.org/tools/single_cell/web/</a>
<b>Other</b>		
20 mL Scintillation Vials, Borosilicate glass, with screw cap, Kimble Chase	VWR	Cat#490007-896
2 mL screw cap vial clear w/wr 12 mm	Agilent Crosslab	Cat#5182-0715
Screw cap 12 mm, blue, PTFE-lined, solid top	Agilent Crosslab	Cat#5183-2075
250ul vial insert, glass with polymer feet	Agilent Crosslab	Cat#5181-1270

**RESOURCE AVAILABILITY**

**Lead contact**

Further information and requests for resources and reagents should be directed to and will be fulfilled by the lead contact, Yehuda Ben-Shahar, [benshahary@wustl.edu](mailto:benshahary@wustl.edu).

**Materials availability**

Fly lines generated in this study are available by request to the lead author.

**Data and code availability**

- All data have been deposited at Mendeley Data and are publicly available as of the date of publication. DOIs are listed in the [key resources table](#).
- All code is available in this paper's [supplemental information](#).
- Any additional information required to reanalyze the data reported in this paper is available from the [lead contact](#) upon request.

**EXPERIMENTAL MODEL AND SUBJECT DETAILS**

Flies were maintained on a standard cornmeal medium under a 12:12 light-dark cycle at 25°C. Unless specifically stated, the *D. melanogaster* Canton-S (CS) strain served as wild-type control animals. UAS-TNT-E, UAS-TNT-IMP-V1-A, UAS-mCD8:GFP, LexAop-myr:GFP, UAS-Red Stinger, Df(1)BSC663, Df(1)BSC754, *Gr8a*-GAL4, *Gr8a*<sup>1</sup>, *desat1*-Gal4, r4-Gal4 and *fruP1*-LexA fly lines were from the Bloomington Stock center. Originally in the *w*<sup>1118</sup> background, the *Gr8a*<sup>1</sup> null allele was outcrossed for six generations into the CS wild-type background, which was used as a control. Likewise, the *desat1*-Gal4 allele was outcrossed for six generations into this *Gr8a* null background. *PromE(800)*-GAL4 and *PromE(800)*>*Luciferase* were from Joel Levine (The University of Toronto, Canada). The following *Drosophila* species were obtained from the San Diego Stock Center (now National *Drosophila* Species Stock Center at Cornell University): *D. simulans* 14011-0251.192, *D. sechellia* 14021-0248.03, *D. yakuba* 14021-0261.01, *D. erecta* 14021-0224.00, *D. ananassae* 14024-0371.16, *D. pseudoobscura* 14011-0121.104, *D. persimilis* 14011-0111.50, *D. willistoni* 14030-0811.35, *D. mojavensis* 15081-1352.23, and *D. virilis* 15010-1051.118. The UAS-*Gr8a* transgenic lines were generated by cloning the *D. melanogaster* and *D. mojavensis* *Gr8a* cDNAs into pUAST-attB vector by using 5' EcoRI and 3' NotI restriction sites, followed by  $\Phi$ C31 integrase-dependent transgenesis at a Chromosome 2 attP landing site (2L:1476459), as previously described.<sup>88</sup> Subsequently, both UAS-*Gr8a*<sup>cDNA</sup> lines were transgressed into the *Gr8a*<sup>1</sup> background, resulting in complete substitution of the endogenous *Gr8a* with expression of a *Gr8a* ortholog. The *ppk23*-LexA line was generated by integrating our previously described *ppk23* promoter DNA fragment<sup>31</sup> into the pBPnlsLexA::p65Uw plasmid,<sup>89</sup> followed by  $\Phi$ C31 integrase-dependent transgenesis as above. For all fly lines, males and females were used. For all experiments, the age of flies used were 4–7 days old.

The GFP-tagged allele of *Gr8a* was generated via CRISPR/Cas9-dependent editing using a modified “scarless” strategy by using the sgRNA CGAGCAAGCGCGGAACGATT and a 3XP3>dsRed in the donor plasmid as a reporter for edited animals as previously described.<sup>90,91</sup> Control lines with matching genetic

backgrounds were established by selecting DsRed-negative injected animals. The final tagged *Gr8a* allele was generated by removing the DsRed cassette via the introduction of the *piggyBac* transposase.<sup>91</sup>

## METHOD DETAILS

### Immunohistochemistry

To visualize the expression pattern of *Gr8a* in males and females, *Gr8a-GAL4* flies<sup>22</sup> were crossed to UAS-CD8::EGFP and live-imaged at 5 days old using a Nikon-A1 confocal microscope. To demonstrate *Gr8a* expression in oenocytes, abdomens from *Gr8a-GAL4/UAS-myr::GFP; PromE(800)>Luciferase* flies were dissected and immunostained as previously described<sup>31,88</sup> by using a Rabbit anti-GFP (1:1000; A-11122, Thermo Fisher Scientific) and a mouse anti-luciferase (1:100; 35-6700, Thermo Fisher Scientific) antibodies followed by Alexa Fluor 488 anti-rabbit and Alexa Fluor 568 anti-mouse secondary antibodies (Both at 1:1000; Thermo Fisher Scientific). To visualize the GR8A protein, abdomens of control flies and flies with CRISPR/Cas9 generated GFP-tagged GR8A were dissected and immunostained as previously described<sup>31,88</sup> using a Rabbit anti-GFP antibody (1:1000; A-11122, Thermo Fisher Scientific) followed by Alexa Fluor 488 anti-rabbit secondary antibody (1:1000; Thermo Fisher Scientific).

### mRNA expression

Newly eclosed flies were separated by sex under CO<sub>2</sub> and aged for 5 days on standard cornmeal medium. On day 6, flies were placed in a -80°C freezer until RNA extraction. To separate body parts, frozen flies were placed in 1.5 mL microcentrifuge tubes, dipped in liquid nitrogen, and then vortexed repeatedly until heads, appendages, and bodies were clearly separated. Total RNA was extracted using the Trizol Reagent (Thermo Fisher Scientific) separately from heads, bodies, and appendages for *Gr8a* expression and from bodies for desaturase enzyme genes. cDNAs were synthesized using Super-Script II reverse transcriptase (Thermo Fisher Scientific) with 500 ng total RNA in a 20 µL reaction. cDNAs were used in endpoint RT-PCR (Table 1) or in Real-time quantitative RT-PCR as previously described with *Rp49* as the loading control gene.<sup>30,31,88,90,91</sup> Primer sequences are described in Tables S1–S3.

### Courtship behavior assays

Single-pair assays were performed as we have previously published.<sup>30,31</sup> In short, newly eclosed males were kept individually on standard fly food in plastic vials (12 × 75 mm). Newly eclosed virgin females were kept in groups of 10 flies. All behaviors were done with 4–7 day-old animals, which were housed under constant conditions of 25°C and a 12h:12h light-dark cycle. Courtship was video recorded for 10 min for male courtship and 15 min for female mating receptivity. Male courtship latency and index were measured as previously described.<sup>30,31</sup> Female receptivity index (copulation latency) was defined as the time from the initiation of male courtship until copulation was observed. If copulation was not observed, the maximum amount of time (900s) was taken as the copulation latency. Unless otherwise indicated, assays were performed under normal light conditions.

Male mate-choice assays were performed in round courtship arenas. Briefly, one *D. melanogaster* virgin female and one interspecific virgin female was decapitated under CO<sub>2</sub> and placed in the arena. One virgin male *D. melanogaster* was then aspirated into the arena and behavior was video recorded for 10 min. The first female courted (by male wing extension) was noted. Male mate-choice assays were performed under red light conditions.

### Perfuming studies

Synthetic compounds were synthesized by J.G.M. Perfuming studies were performed using a modified protocol from.<sup>24</sup> In short, for exaggerated CHC transfer assays, 3 mg of each compound was dissolved in 6 mL hexane (Sigma-Aldrich #139386-500 ML), for a working solution of 0.5 mg/mL. For biologically relevant transfer assays, a working solution of 1600 ng/mL, 40 ng/mL, and 640 ng/mL in hexane were used for 7-C<sub>25</sub>, 7-C<sub>27</sub>, and 9-C<sub>25</sub>, respectively. 0.5 mL of working solution was pipetted into individual 2 mL glass vials fitted with 12 mm PTFE lined caps (Agilent Crosslab, 5182-0715, 5183-2075). The hexane was evaporated under a nitrogen gas flow, such that a residue of the compound was left around the bottom one-third of the vial. Control vials were prepared using hexane without a spiked compound. Vials were kept at -20°C until use. Flies used in these trials were collected as described above, kept in single sex groups and aged for 4 days on standard cornmeal medium at 25°C. 24 h before perfuming, 20 flies of one or the other sex were placed in glass vials containing standard cornmeal medium (12 × 75 mm). To perfume

the flies, these groups of 20 flies were dumped without anesthesia into each 2 mL vial containing the compound of interest, and were vortexed at medium-low speed for 3 pulses of 20 s punctuated by 20 s rest periods. Flies were transferred to new food vials and were allowed to recover for 1 h. Perfumed flies were then used in 10–15 min courtship behavior assays as described above and the remaining flies were used in pheromone analyses to verify compound transfer. In cases where copulation was not observed, the maximum amount of time (900 s) was taken as the copulation latency. The genotype of flies that were perfumed differed based upon the genotype with the lower amount of each compound as determined in Figures 4B, 4C, and 4F). In all cases, compound transfer was verified by CHC extraction and GC/MS (Table S4). For biologically relevant CHC transfer assays, we were unable to successfully transfer a biologically relevant amount of 9-C<sub>25</sub>, so these assays were omitted from analysis.

### Phylogenetic analysis

Protein sequences of GR8A orthologs from the 12 sequenced *Drosophila* reference genomes were aligned by using the ClustalW algorithm in the Omega package,<sup>87</sup> followed by ProtTest (v2.4) to determine the best model of protein evolution.<sup>86</sup> Subsequently, Akaike and Bayesian information criterion scores were used to select the appropriate substitution matrix. We then used a maximum likelihood approach and rapid bootstrapping within RAxML v 7.2.8 Black Box on the Cipres web portal to make a phylogenetic tree.<sup>92</sup> Visualizations of the bipartition files were made using FigTree v1.3.1 (<http://tree.bio.ed.ac.uk/software/figtree/>).

### Pheromone analysis

Virgin flies were collected upon eclosion under a light CO<sub>2</sub> anesthesia and kept in single-sex vials in groups of 10 with 6 biological replications for each genotype and sex. Virgin flies were aged for 5 days on standard cornmeal medium at 25°C. To collect mated flies, both females and males were aged for 3 days before single mating pairs were placed in a standard fly vial with standard cornmeal food for 24 h. The pair was then separated for 24 h before collection. Copulation was confirmed by the presence of larvae in the vials of mated females several days later. On the morning of day 5, flies were anesthetized under light CO<sub>2</sub> and groups of five flies were placed in individual scintillation vials (VWR 74504-20). To extract CHCs, each group of flies was covered by 100  $\mu$ L hexane (Sigma-Aldrich #139386-500 ML) containing 50  $\mu$ g/mL hexacosane (Sigma-Aldrich #241687-5G) and was washed for 10 min. Subsequently, hexane washes were transferred into a new 2 mL glass vial containing a 250  $\mu$ L insert (Agilent Crosslab 5181-1270) and were stored at –20°C until shipment to the Millar laboratory.

Analyses of CHC profiles were done by gas chromatography and mass spectroscopy (GC-MS) in the Millar laboratory at UC Riverside as previously described.<sup>19</sup> Peak areas were measured, and data was normalized to known quantity of internal standard hexacosane (Sigma-Aldrich #241687-5G). The relative proportion of each compound in each sample was calculated and used in further statistical analysis.

### QUANTIFICATION AND STATISTICAL ANALYSIS

All statistical analyses were performed in R (v 4.2.0).<sup>93</sup> Sample size (n) for each experiment is reported in figure legends. For all analyses, assumptions were checked before statistical analysis. See code in paper's supplement for R analysis. The following functions were used in the base statistics package: `shapiro.test()` (Shapiro-Wilk Normality Test), `fligner.test()` (Fligner-Killeen Test of Homogeneity of Variances), `t.test()` (Student's t test), `wilcox.test()` (Mann-Whitney Rank-Sum Test), `aov()` (ANOVA), `TukeyHSD()` (Tukey's HSD post hoc test), `Kruskal.test()` (Kruskal-Wallis test), `chisq.test()` (Pearson's Chi-squared test). Kruskal-Wallis post hoc was performed using the `kwAllPairsDunnTest` function in the `PMCMRplus` package.<sup>94</sup> Qualitative CHC data were analyzed through a permutation MANOVA using the `adonis` function in the `vegan` package of R with Bray-Curtis dissimilarity measures.<sup>95</sup> CHC profile data were visualized using non-metric multidimensional scaling (`metaMDS`) function in the `vegan` package of R<sup>95</sup> using Bray-Curtis dissimilarity, and either 2 or 3 dimensions in order to minimize stress to <0.1.